2013

Evaluation of the Newburg Sandstone of the Appalachian Basin as a CO2 Geologic Storage Resource

Jack Eric Lewis
West Virginia University

Evaluation of the Newburg Sandstone of the Appalachian Basin as a CO_2 Geologic Storage Resource

Jack Eric Lewis

Thesis submitted to the Eberly College of Arts and Science at West Virginia University

in partial fulfillment of the requirements for the degree of

Master of Science in Geology

Thesis committee:

Dr. Timothy Carr, PhD, WVU, Chair

Dr. Jaime Toro, PhD, WVU

Dr. Ronald McDowell, PhD, WVGES

Morgantown, West Virginia 2012

Keywords: Newburg Sandstone, CO2, Appalachian Basin, Sequestration, Storage, Silurian

ABSTRACT

Evaluation of the Newburg Sandstone of the Appalachian Basin as a CO_2 Geologic Storage Resource

Jack Eric Lewis

The West Virginia Division of Energy is currently evaluating several deep saline formations in the Appalachian basin of West Virginia, which may be potential carbon dioxide (CO_2) sequestration targets. The Silurian Newburg Sandstone play, developed in the 1970's, primarily involves natural gas production from reservoir rock with well-developed porosity and permeability. High initial pressures encountered in early wells in the Newburg indicate that the overlying Silurian Salina Formation provides a competent seal. Due to the large number of CO_2 point sources in the region and the favorable reservoir properties of the formation; including an estimated 300 billion cubic feet (bcf) of natural gas production, a serious evaluation of the Newburg Sandstone may expand our available targets for geologic storage of CO_2. Within the Newburg play, there are several primary fields separated geographically and geologically by salt water contacts and dry holes. Previous studies have determined the storage potential within these individual fields. This study will show that the Newburg is more suitable for small-scale injection tests, instead of large-scale, regional storage operations.

TABLE OF CONTENTS

ACKNOWLEDGEMENTS

I would like to thank my family, especially my mother, for being incredibly supportive throughout my academic and professional career.

I would also like to express my gratitude towards my committee members, in particular Dr. Tim Carr, for his guidance and contributions to this project, and Dr. Ronald McDowell, who has served as an excellent mentor during my tenure at the West Virginia Geological and Economic Survey.

This project would not have been possible without funding from the West Virginia Division of Energy and the Midwest Regional Carbon Sequestration Partnership.

Finally, I would like to thank Katharine Lee Avary and my colleagues at the West Virginia Geological and Economic Survey for always being willing to answer any of my questions, no matter how ridiculous, at the drop of a hat. Your patience is appreciated.

LIST OF FIGURES

Page

1.0 INTRODUCTION

As the industrial world's demand and consumption of fossil fuels continue to grow, so too will the volume of anthropogenic greenhouse gas emissions. Although there are natural sources of carbon dioxide (CO_2) in the earth's atmosphere, human activities, such as the combustion of fossil fuels for electricity consumption, transportation, and industrial purposes, have a significant impact on the atmosphere's concentration of CO_2. Emissions of greenhouse gases continue to rise from a pre-Industrial Revolution concentration of CO_2 in the atmosphere of around 275 parts per million (ppm) to 390.5 ppm CO_2 (Conway and Tans, 2012). With an annual increase of 1-3 ppm, we are rapidly approaching 450 ppm and a possible global temperature increase of 2-3.5^{o} C (IEA, 2011).

Fossil fuel consumption at power plants accounted for 40 percent of total CO_2 emissions in 2008 (Figure 1.1) (McArdle *et al.*, 2002; Conti *et al.*, 2012). As a significant contributor to these greenhouse gases, the United States has also become a leader in studying the effects of these releases into the atmosphere. Considering that human consumption of fossil fuels will continue through this century, technologies are being developed to manage increasing CO_2 emissions. A potential technology, carbon capture and storage, involves the injection and geologic storage of CO_2 emissions into deep geologic formations. Carbon capture and storage has been receiving considerable attention in recent years. In order for carbon capture and storage to be viable, the necessary capture, transportation and infrastructure must be established, as

well as the selection of a geologic storage site with the characteristics necessary for long-term storage (i.e., capacity, injectivity, and containment).

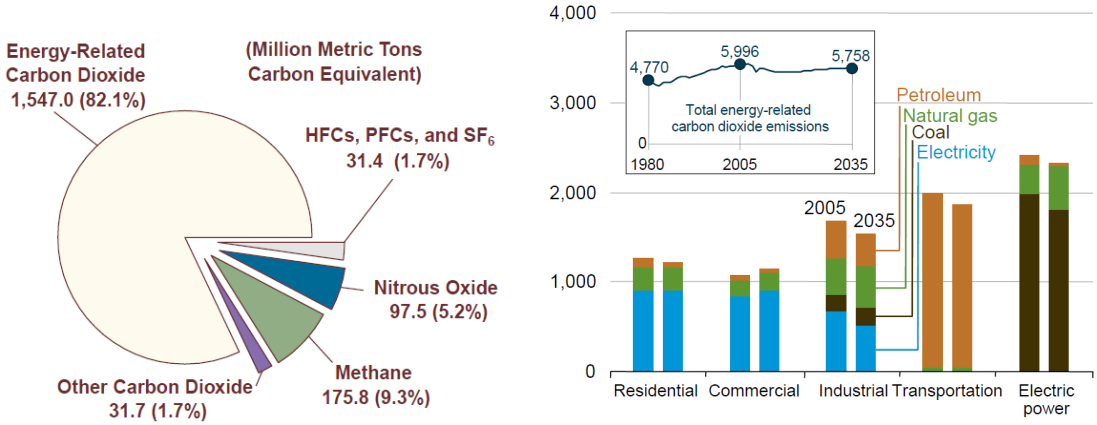

Figure 1.1 CO_2 from fossil fuel combustion makes up 82% of all GHG emissions released into the atmosphere; most of which are the result of electricity generation (Source: McArdle *et al.*, 2002 and Conti *et al.*, 2012).

In an effort to combat the effects that these emissions may have on Earth's atmosphere, one technique that has been proposed involves injecting CO_2 emitted from power plants into deep geologic storage sites. Ideal formations typically are oil reservoirs, in which injected CO_2 can enhance oil recovery, abandoned gas fields, or deep saline formations (Gibbins and Chalmers, 2008). Pressurizing the CO_2 to a supercritical state, in which it is neither considered to be a liquid or gas, increases its density and therefore, increases the amount of CO_2 that can be stored in a given volume. However, assuming hydrostatic pressure and a typical geothermal gradient of 25º C km^{-1} worldwide (Tissot and Welte, 1978), in order for the CO_2 to remain in a supercritical state, geologic

storage targets must be at depths greater than or equal to 800 meters (2600 feet) deep (Figure 1.2) (WVCARB, 2008).

Not only are deep saline aquifers plentiful throughout the United States, but they can trap the CO_2 in several ways (Figure 1.3). Residually, the CO_2 can be trapped in the pore spaces of the rock. It can also dissolve into the formation waters and, over time, react with existing minerals within the formation to form precipitates, which eventually adhere to the surface of individual grains (MRCSP, 2010).

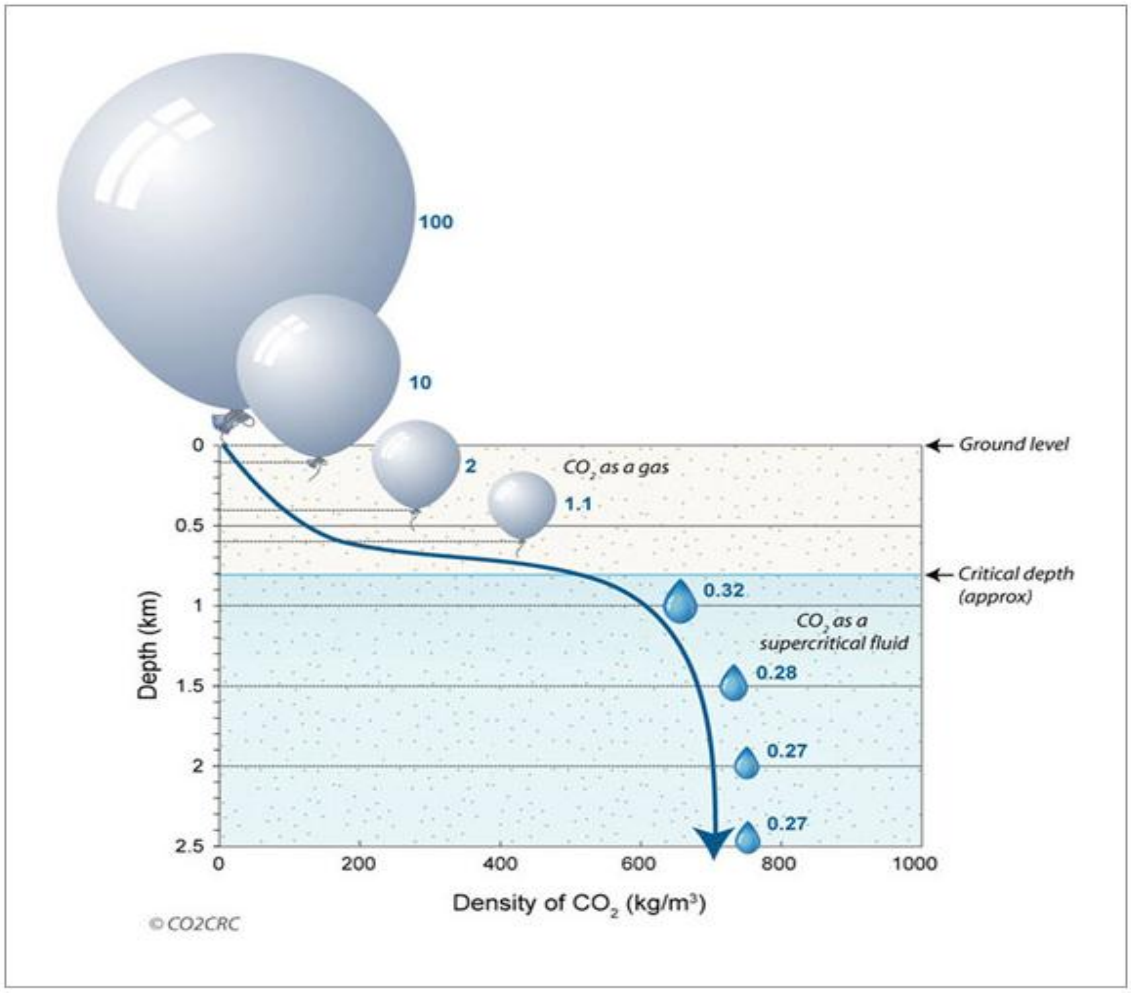

Figure 1.2 CO_2 increases in density with depth and becomes a supercritical fluid CO_2 at depths below 2600 feet (800 m) under hydrostatic pressure. Supercritical fluids take up much less space, and diffuse better than either gases or ordinary liquids through the tiny pore spaces in storage rocks. The blue numbers in this figure show the volume of CO_2 at each depth relative to a volume of 100 kg/m^3 at the surface (Source: WVCARB, 2008).

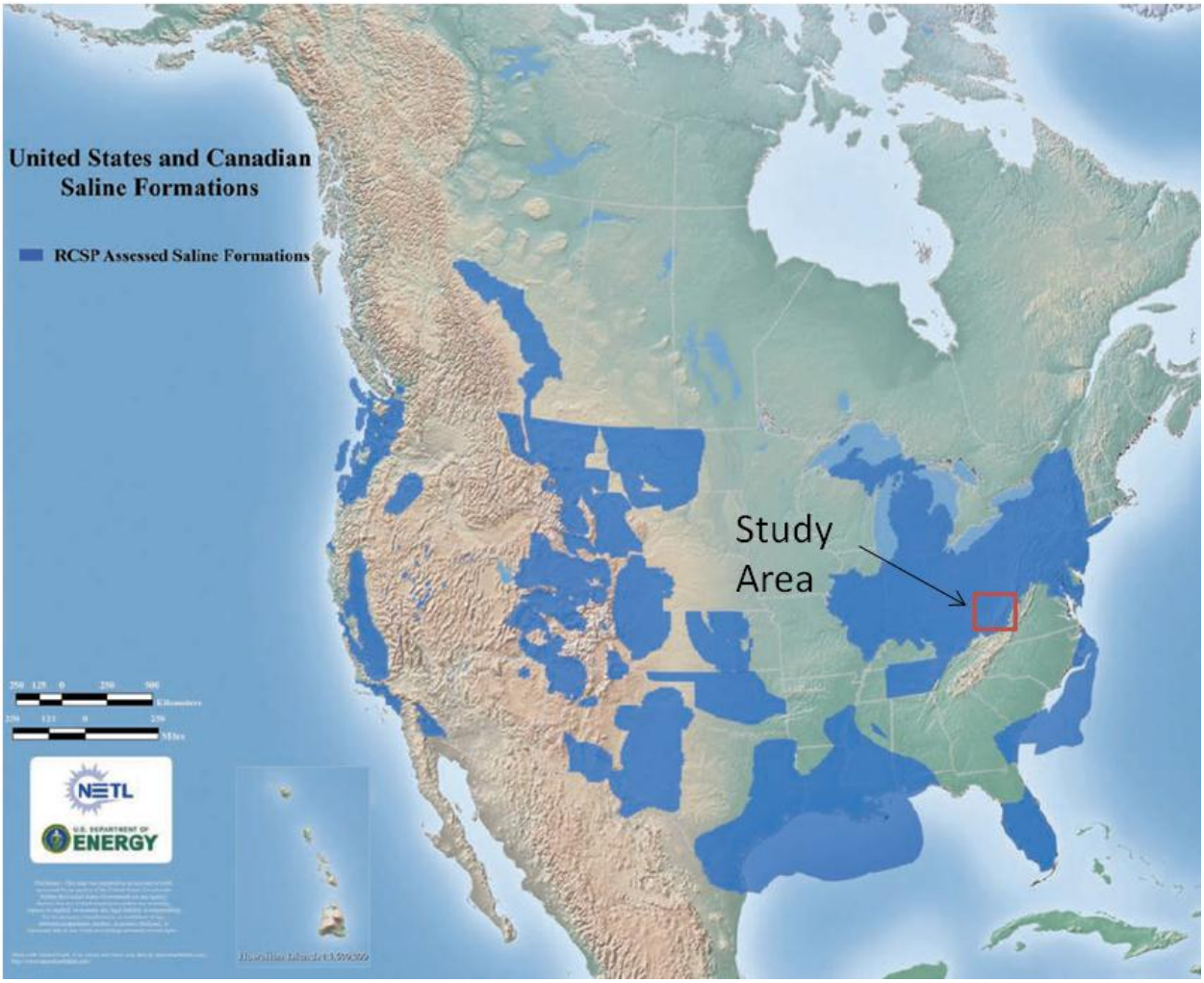

Figure 1.3 Map showing location of major, deep saline aquifers (in blue) throughout the United States and general location of the study area (Modified from DOE/NETL, 2010).

In order to insure the long-term containment of the CO_2 once it has been injected, there must be an overlying formation with low permeability to prevent upward migration into other, less stable formations and possibly into freshwater aquifers or the atmosphere. In addition, a trapping mechanism, in relation to the structural or stratigraphic sequence in a given area, must be present to inhibit lateral migration of the fluid. This study will show that the Upper Silurian Newburg Sandstone, a tight, fractured unit that is a gas

producing anticlinal play (Patchen, 1996), possesses characteristics necessary for CO_2 injection testing and is a significant CO_2 geologic storage resource.

2.0 REGIONAL GEOLOGY

The Silurian Newburg Sandstone play, developed during the 1960's and 1970's, primarily involves natural gas production from reservoir rock with well-developed, matrix and fracture porosity and permeability. Several fields within the play make up the majority of the production in western and south-central West Virginia including the North and South Ripley fields, Rocky Fork and Cooper Creek fields and the Kanawha Forest field (Figure 2.1) (Patchen, 1996). Present across central West Virginia, the subsurface unit referred to by drillers as the "Newburg" separates the evaporite of the overlying Salina Formation from carbonate of the McKenzie Formation or the Lockport Dolomite (Figure 2.2). Sourced from erosion of the Taconic uplifts in the east, Woodward (1959) and Overbey (1961) determined the stratigraphic equivalent of this marine deposit to be, in part, the Williamsport Sandstone. In outcrop, the Williamsport is a silica-cemented quartz sandstone that has been slightly metamorphosed. The brittleness of the formation gives it a blocky, fractured appearance, similar to the Silurian Tuscarora Sandstone. However, it is much thinner than the Tuscarora with thickness between 20 and 40 feet (6 and 12 meters) in outcrop and up to 50 feet (15 meters) in the subsurface.

Examination of several cores taken in the Newburg suggests the lithology is more similar to portions of the Wills Creek Formation, which overlies the Williamsport, and consists of carbonate cemented sand, shale and evaporite deposits (McDowell *et al.*, 2007). There appears to be some confusion in stratigraphic terminology when referring to the sandstone that underlies the Wills Creek Formation. Patchen (1996) notes that the term “Crabbottom” was first used by Swartz and Swartz (1940) to describe a thick sandstone, situated between the Wills Creek Formation and the McKenzie “Limestone”, in specific areas along the West Virginia/Virginia border. Later correlations determined this outcrop unit to be equivalent to the Newburg Sandstone (Patchen, 1996). However, it should be noted that Swartz and Swartz (1940, abstract p. 2008) described the Crabbottom as a “thick-bedded, whitish sandstone at the base of the Wills Creek formation”. The type section for this is located approximately two miles (three kilometers) east of the settlement of Blue Grass, Virginia (formerly known as Crabbottom) on Highland County Highway 642. According to Diecchio and Dennison (1996), this unit is the Williamsport Sandstone. The National Geologic Map Database (NGMDB) (2012), managed by the United States Geological Survey (USGS), does not recognize the Newburg or the Crabbottom as a valid stratigraphic unit.

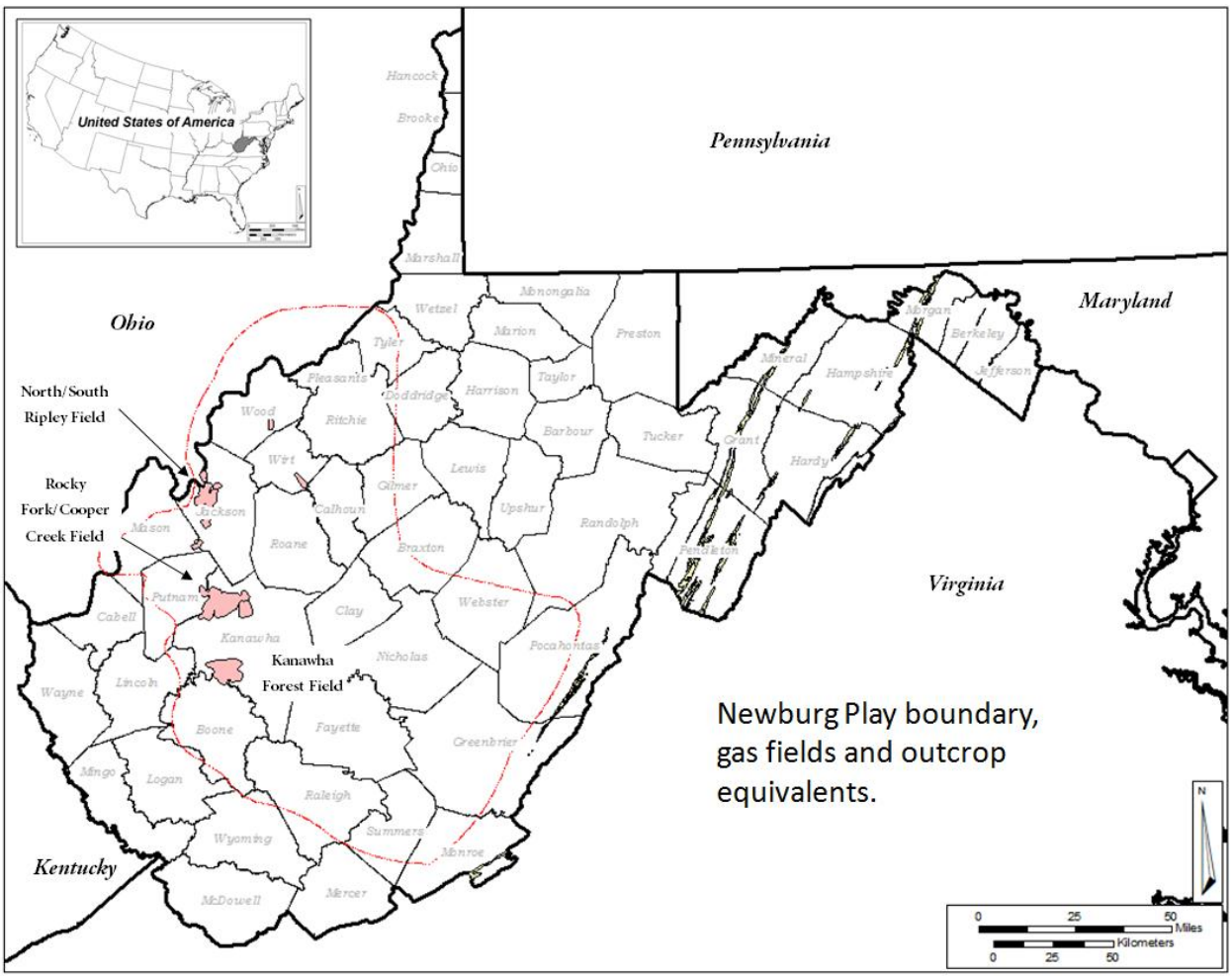

Figure 2.1 Boundary of the Newburg Sandstone play in West Virginia and the three major producing gas fields and outcrop equivalents of the Newburg Sandstone (data collected from WVGES database, updated 2012).

Most fields in the Newburg are a combination of structural and stratigraphic traps separated by down-dip salt water contacts or low porosity rocks. Uncharacteristically over-pressured compared to most gas fields in the Appalachian basin, six to seven years appears to be the average life span of Newburg wells (Patchen, 1996). This suggests well-developed porosity and permeability, especially in the pay zone, which is normally in the middle to upper section of the Newburg interval. The major producing

fields are at least 5,000 feet deep and recorded initial pressures greater than 2000 psi (pounds per square inch) (Patchen, 1996). These pressures appear to be good indicators of the Newburg's ability to retain fluids once injected and long-term CO_2 containment should not be a problem as long as the storage pressure does not exceed hydrostatic pressure.

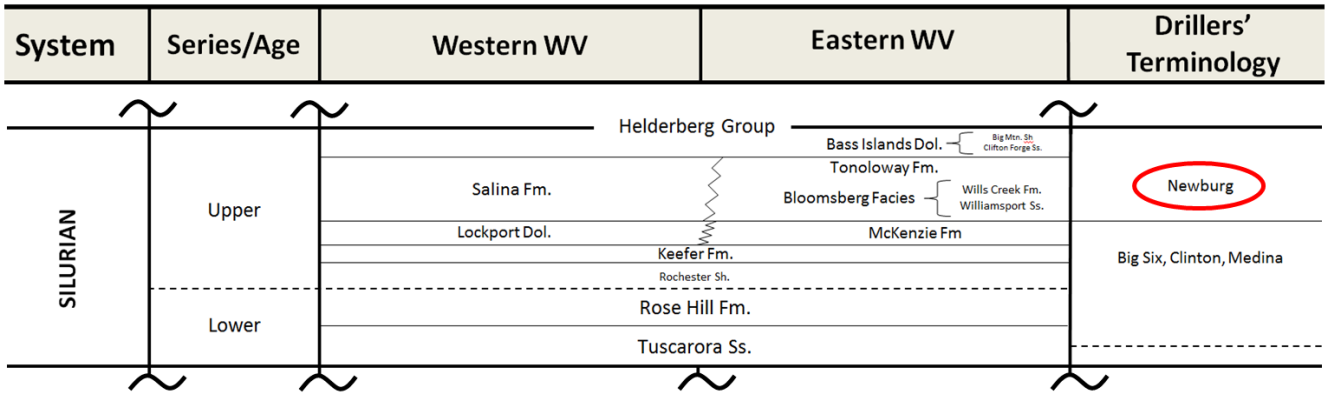

Figure 2.2 Generalized stratigraphy of the Silurian in West Virginia with the Newburg Sand highlighted (modified from WVGES, 2012).

As the Newburg play was being developed in the 1960's, four rig hands died from H_2S inhalation while working under the derrick floor. Initially thought to be sourced in the Newburg itself, it was later determined that the source of this poisonous gas was a thin zone, several hundred feet above the Newburg, in the Salina. It was mentioned as "sour gas" or "black water" on early completion records (Patchen, personal communication 2012). Gases with high sulfur conditions are not surprising in an evaporite sequence and we see indications of evaporite deposition in the Wills Creek Formation in the form of gypsum in the core and outcrop. Gypsum and halite casts

were observed in the Bluegrass outcrop of the Wills Creek Formation but not in the underlying Williamsport Sandstone in eastern West Virginia (Figure 2.3).

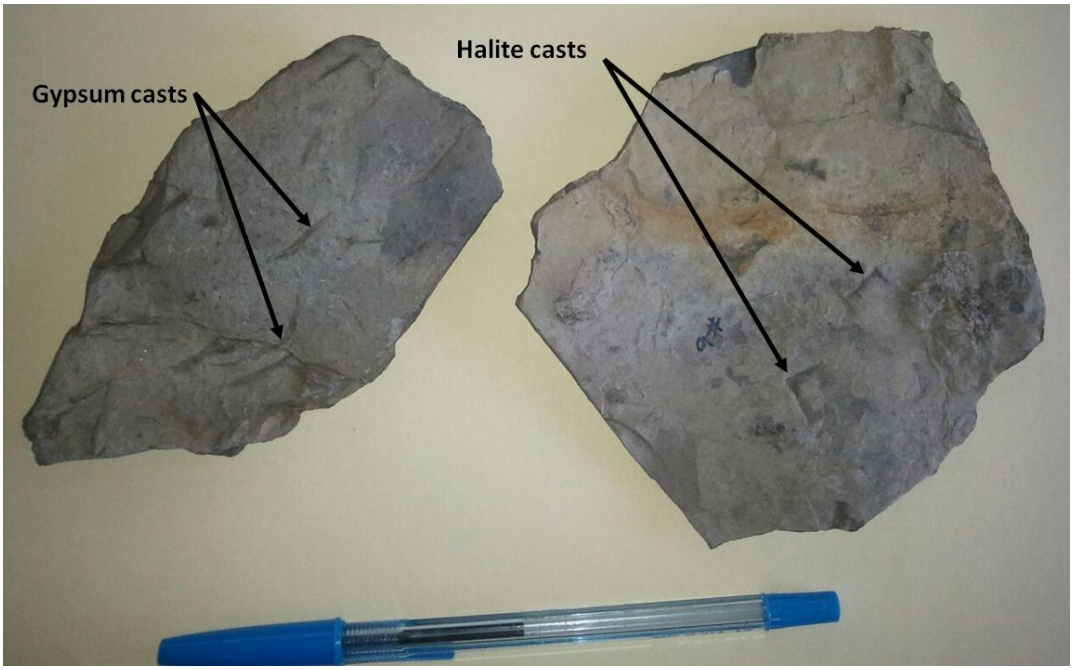

Figure 2.3 Outcrop sample of calcareous siltstone from the Wills Creek Formation containing casts of gypsum and halite. Location is approximately two miles east of Bluegrass, Virginia, on the northeast side of Virginia Route 642, west of U.S. Route 220 in Highland County, Virginia (Samples from section described by Diecchio and Dennison, 1996).

Natural gas from the Newburg was first discovered in the 1939, but it wasn't until the middle of the 1960's that production increased to significant quantities (Patchen, 1996). Production statistics from the West Virginia Geological and Economic Survey (WVGES) are available only starting in 1979 (Figure 2.4). The early 1980's and 1990's saw spikes in annual production reaching almost three billion cubic feet (3 bcf) followed by a general decline to approximately 500 million cubic feet (500 mmcf) in 2010 (Figure 2.4).

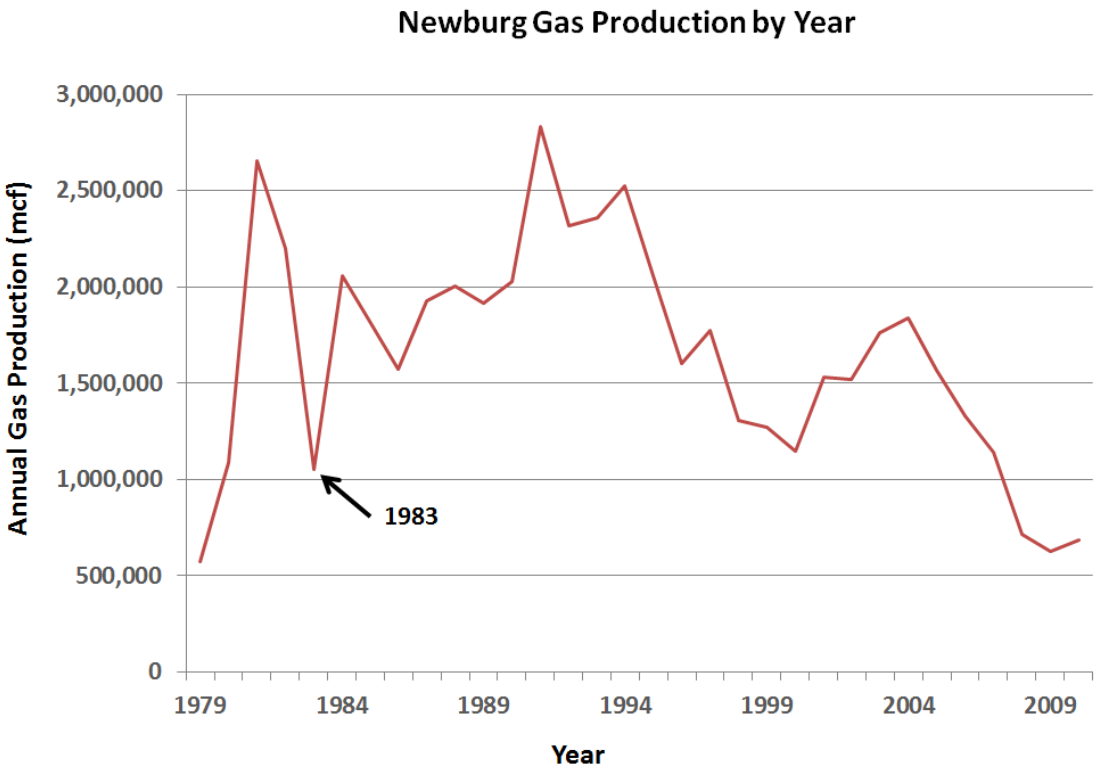

Figure 2.4 Graph showing annual gas production from reservoirs in the Newburg Sandstone (WVGES database, updated 2012). In 1983, there were issues with reporting among state agencies; therefore, an anomalous dip in production is shown for that year.

2.1 Depositional History

Through much of the Silurian, the West Virginia area was predominantly a seaway extending to open ocean to the south-west (Figure 2.5). Baltica collided with North America during the Taconic orogeny closing off the seaway, and forming an epiric sea, with shallow, highly saline, evaporitic conditions (Figure 2.5). Initial constriction of the seaway, during the Early Silurian, increased wave energy into the basin resulting in

high-energy marine deposits in southwest West Virginia. The facies relationship between the marine deposits of the Newburg Sandstone, the siliciclastic deposits of the Williamsport Sandstone and the evaporite deposits of the Wills Creek Formation shows the gradual restriction of the seaway during the Silurian. Once cutoff from wave action, a shallow basin formed with evaporite deposits of the Salina Formation (Smosna and Patchen, 1978). These Upper Silurian evaporite deposits provide a major regional seal that forms traps in Newburg Sandstone gas reservoirs, and provides the regional seal for containment and the potential for long-term geologic storage of CO_2.

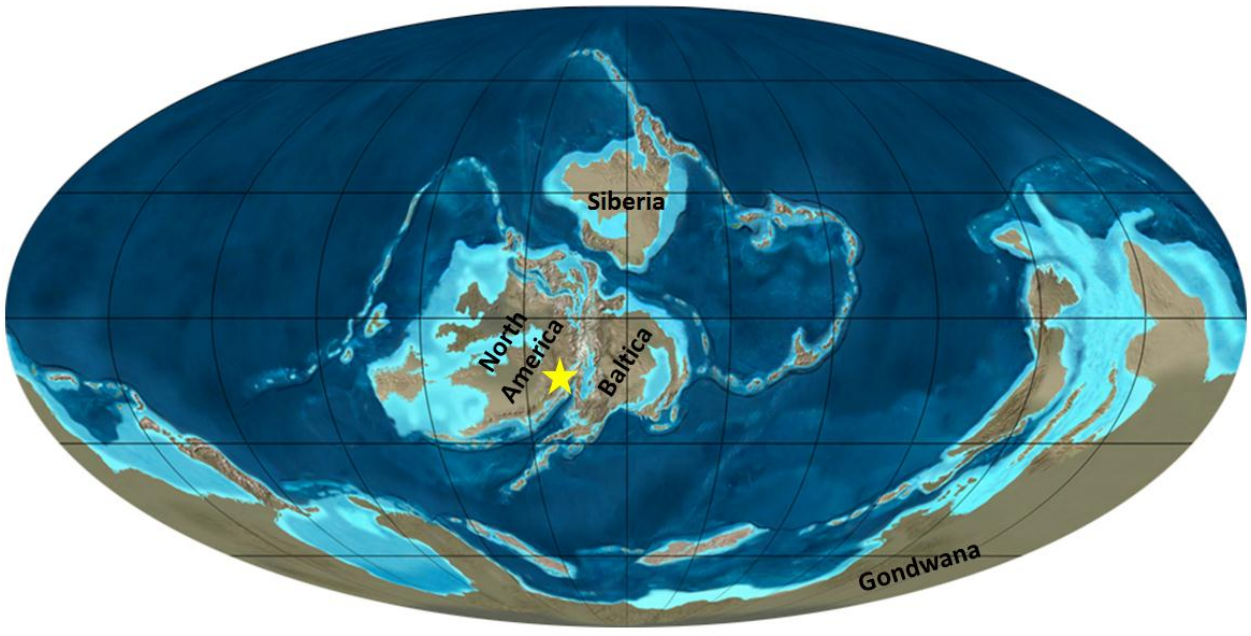

Figure 2.5 Global paleogeography during depostion of Silurian sequences (modified from Blakey, 2011). In the early Silurian, the seaway is open to the ocean and becomes restricted forming an evaporitic basin during the Late Silurian as a result of the Taconic Orogeny. General location of study area indicated by yellow star.

The traditional depositional model of the Newburg includes elements such as barrier islands, lagoons, and tidal marshes (Patchen, 1996). Reworking of sediments implies high energy settings on a shallow shelf complete with sandstone units deposited in ebb and flood tidal deltas, lagoons, washover fans, and tidal deposits. Deposition is interpreted to be a result of both wind and wave processes (Patchen, 1996) (Figure 2.6).

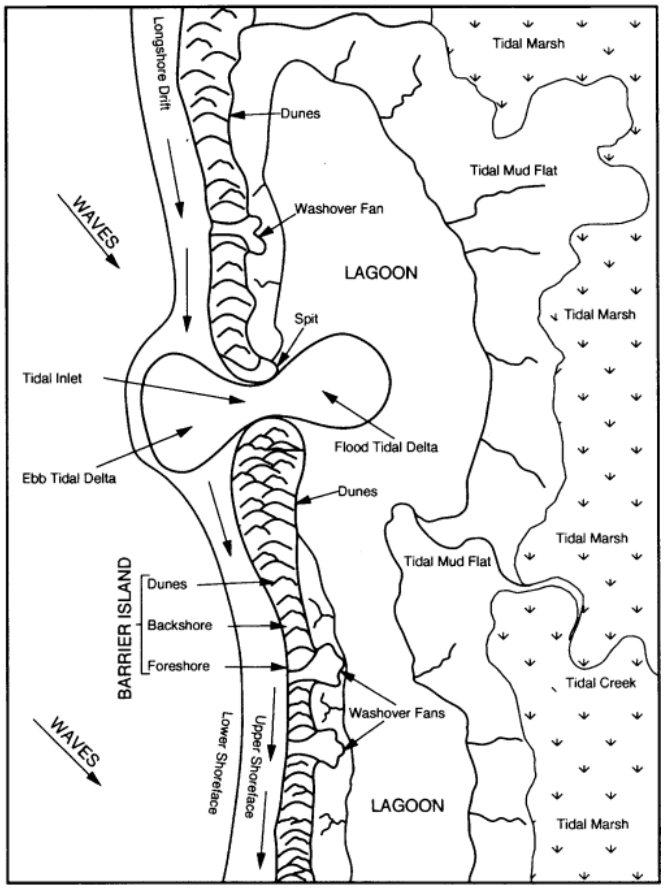

Figure 2.6 Traditional depositional model for the Newburg Sandstone showing the mix of barrier islands, tidal deltas, lagoons, washover fans and tidal deposits (Patchen, 1996).

2.2 Structural Setting

A majority of the thrusting in West Virginia is located east of the Appalachian plateau and therefore, east of major petroleum production. In western West Virginia, normal faulting is the dominant structure in Precambrian-aged basement rocks. West of the Appalachian mountains, the majority of faults in the Devonian Onondaga Limestone are inferred to be “normal” except in the Burning Springs area in western West Virginia, where reverse and thrust faults extend into the Devonian and younger rocks, and are responsible for the formation of a geologic anomaly known as the Burning Springs anticline (Figure 2.7). Small thrust faults exist throughout the Devonian shales throughout the state.

The Wood 351 well (API# 4710700351), one of only a few deep wells in West Virginia reported 1,527 feet (465 m) of repeated section between the Newburg Sandstone and the Oriskany Sandstone (Cardwell, 1971). This anomaly has been determined be a result of thrust faulting, but it has not been associated with a particular orogeny (Cardwell, 1971).

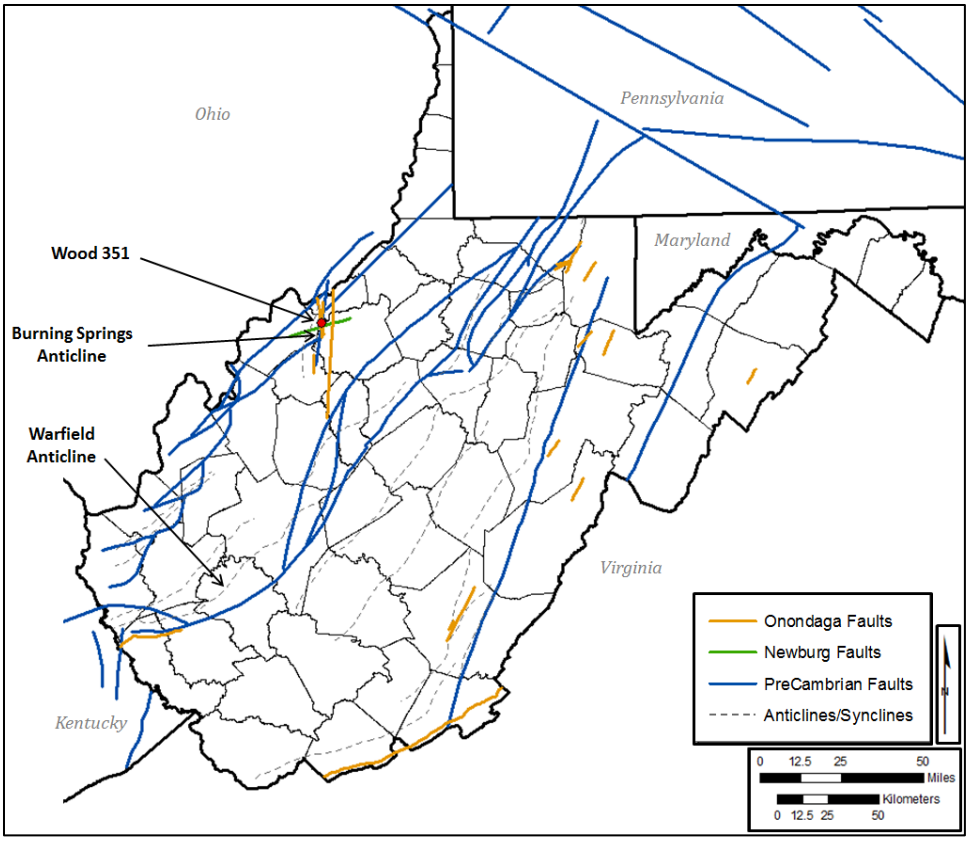

Figure 2.7 Major faults and structure elements recognized by the West Virginia Geologic and Economic Survey. Generally, thrusting and reverse faulting is confined to eastern West Virginia and normal faulting dominates to the west. However, in the Burning Springs area, the Wood 351 well is described as having a significant amount of repeated section, beginning in the Lower Silurian attributed to thrust faulting. This, in addition to regionally anomalous thrusting in younger, Devonian/Carboniferous rocks, led to the formation of the Burning Springs Anticline (WVGES database, updated 2012).

3.0 PREVIOUS AND RELATED WORK

WVGES has released several publications that refer to the Bloomsberg facies in outcrop. The earliest such release was in the 1924 Mineral and Grant County Report (Reger and Tucker, 1924). Although Stout *et al.* (1935) is credited for first using the term, the name "Newburg" did not make an appearance in WVGES publications until Haught (1959) noted the name on well logs. In addition to core descriptions, correlations and mapping, Patchen was involved in distributing information about the development of the Newburg gas fields in a series of American Association of Petroleum Geologists (AAPG) publications from the late 1970's through the 1980's (Lytle *et al.* 1972, 1973, 1974, 1975, 1976, and 1977; Patchen *et al.*, 1978, 1979, 1980, 1981, 1982, 1983, 1984, 1985, 1986, 1987, 1988, 1989, and 1990). Most notably, his preliminary report chronicled the early stages of development within the play (Patchen, 1967). Cardwell (1971) devoted an entire publication to the Newburg Sandstone in which he discussed the characteristics of the individual gas fields and overall history of the development of the unit as a viable gas play. Woodward (1941) compiled the first full report of the entire Silurian column. Russell (1972) included the Newburg in his discussion of "pressure-depth" relations in the Appalachian region. Smosna and Patchen (1978) described the evolution of the Appalachian basin throughout the Silurian. Several studies have been conducted on the Warfield anticline, including Gao and Shumaker's (1996) study of its impacts on hydrocarbon exploration. As part of the Midwest Regional Carbon Sequestration Partnership (MRCSP), funded by the United States Department of Energy (U.S. DOE), potential sequestration volumes of individual gas fields were calculated (WVGES, 2005).

4.0 METHODOLOGY AND DATA SET

Technical storage capacity for the Newburg Sandstone is calculated using the following equation:

$$\mathbf{G_{CO2} = A\ h_g\ \phi_{tot}\ \rho\ E}\ \text{(USDOE, 2012)} \qquad \mathbf{(1)}$$

G_{CO2} is an estimation of the CO_2 in metric tons (tonnes) that can potentially be stored within a particular unit, **A** is the geographical area in square feet being assessed, $\mathbf{h_g}$ is the gross thickness in feet of the target formation, $\boldsymbol{\phi_{tot}}$ is the decimal average porosity of the entire unit being assessed, $\boldsymbol{\rho}$ is the density of CO_2 in pounds per cubic foot (lbs/ft^3) expected at pressure and temperature conditions represented by the particular rock unit in pounds per cubic feet, and **E** is the storage efficiency factor that represents the percentage of the total pore volume filled by CO_2. This factor is a P_{10}, P_{50}, and P_{90} confidence interval that takes into account any barriers which may inhibit CO_2 from accessing all of the pore space in the formation and uses values of .51%, 2.0%, and 5.5%, respectively (USDOE, 2012). The result is divided by 2200 to convert from pounds to tonnes (metric tons).

Out of over 800 wells within the Newburg play, 102 had geophysical logs through the Newburg containing the following suite of logs: Gamma Ray (GR), Density Porosity (DPHI) and Neutron Porosity (NPHI). The areal extent of these 102 wells defines the

study area (Figure 4.1). GR logs were used in conjunction with the porosity logs for correlation purposes. DPHI and NPHI logs were used to calculate the average porosity (ϕ_{tot}) throughout the interval.

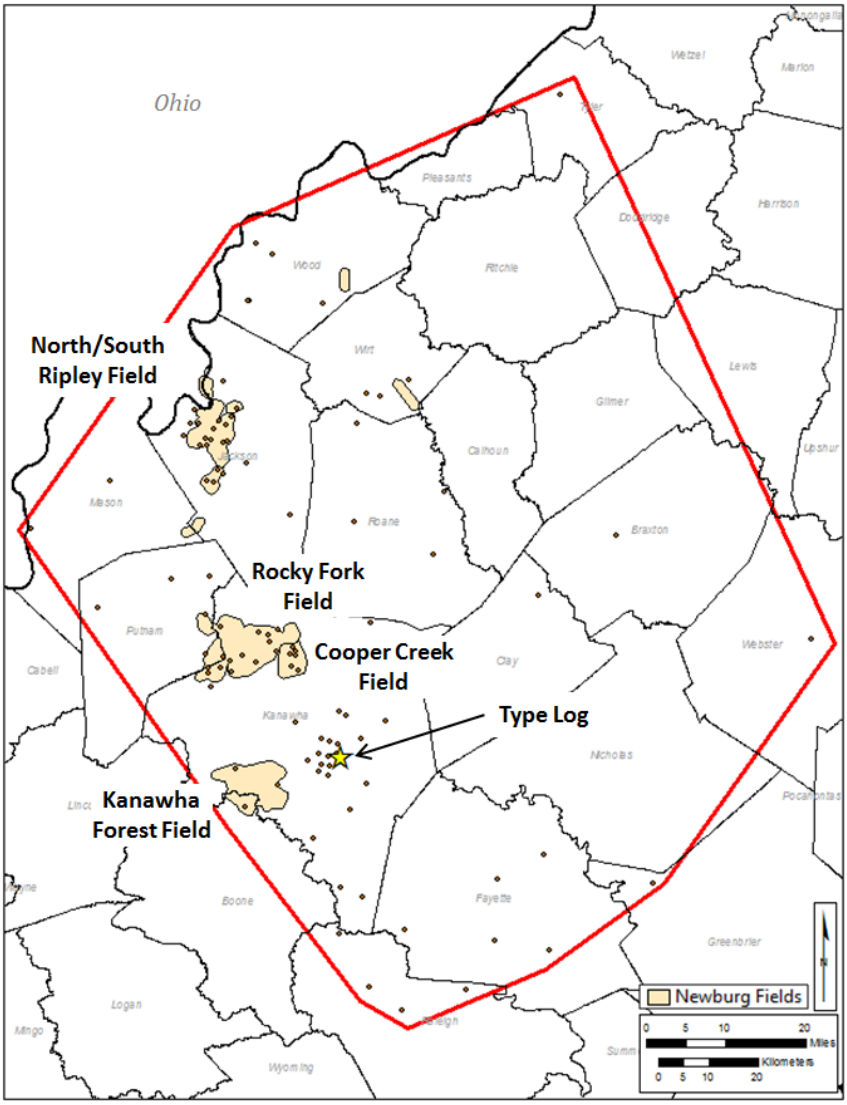

Figure 4.1 Map of study area, Newburg fields, locations of 102 wells used in calculations and location of type log (star) that comes from the Kan and Hocking C&C #20653 well (API# 4703903646) located in Kanawha County, West Virginia.

The type log used for this study comes from the Kan and Hocking C&C #20653 well (API# 4703903646), located in Kanawha County, West Virginia. This is a non-productive well targeting the lower Silurian Tuscarora Sandstone. Typically, the Newburg is identified on well logs by a characteristic porosity response in the middle to upper zone of the interval. This response is recognized by a dramatic increase in the DPHI curve that crosses over and surpasses the NPHI values. In relatively clean lithology (low clay content indicated by low gamma-ray values), such as the Newburg Sandstone, the crossover of DPHI and NPHI is indicative of gas in the pore space instead of liquids such as brine or oil. Without the density and neutron curves, it can be difficult to distinguish the Newburg Sandstone from the overlying Salina Group and underlying McKenzie Formation (Figure 4.2a). The low gamma ray values on the type log show predominantly clean carbonate and sandstone through the Newburg with a couple of shale zones appearing towards the bottom of the interval as reflected by high gamma ray values. The negative DPHI values above and below the Newburg are good indicators of denser minerals such as anhydrite, typical of the overlying Salina evaporite sequence (Figure 4.2a) (Asquith and Krygowski, 2004). After digitizing the type log, NPHI and DPHI values were "normalized" to eliminate negative values and averaged to create NORM_PHIA, or the amount of gas filling the pore space. Using Petra™ software, water saturation (S_W) was calculated and multiplied by NORM_PHIA to create Bulk Volume of Water (BVW) which reflects the amount of water filling the pore space (Figure 4.2b). BVW and NORM_PHIA were then plotted together and shaded red and blue to reflect the amount of hydrocarbons and water filling the pore space respectively (Figure 4.2b). Even though the type log shows cross-over indicative of gas at the top of

the formation, a Pickett Plot shows that between a third and a half of the pore space within the top five feet of the Newburg is filled with water, while water takes up a majority of the pore space in the rest of the formation (Figure 4.2c). A closer look at the log allows one to determine where these zones are with respect to depth (Figure 4.2 a and b.).

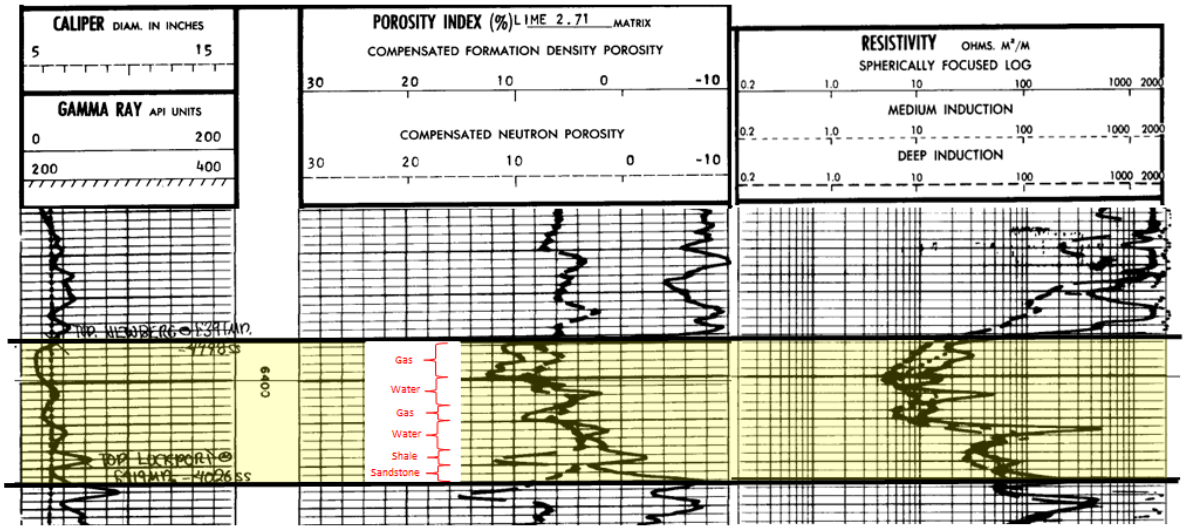

Figure 4.2a

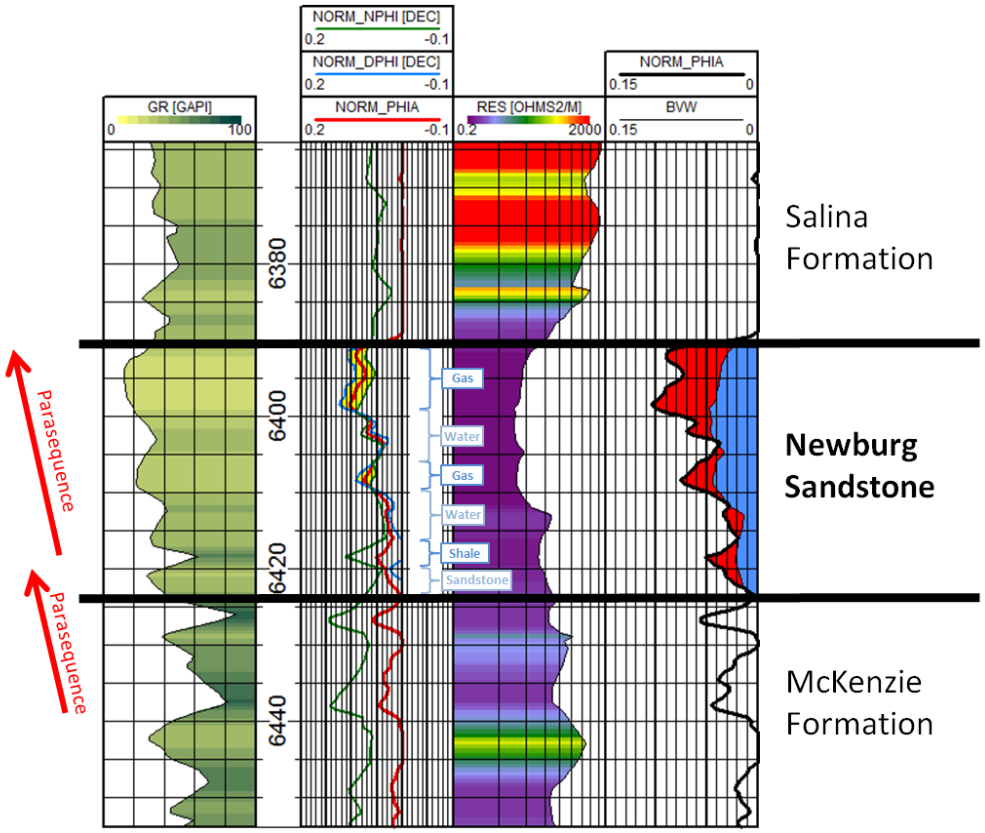

Figure 4.2b

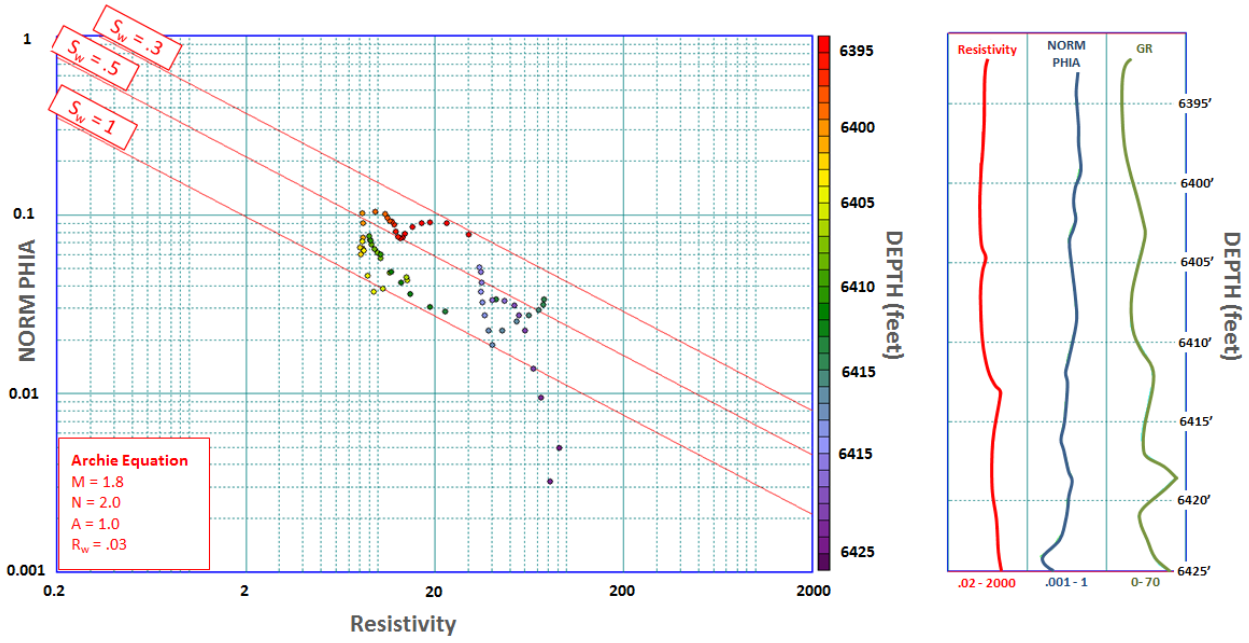

Figure 4.2c

Figure 4.2 a. Type log, Kanawha County, API# 4703903646. Newburg highlighted in yellow. **b.** Type log digitized. NPHI and DPHI values were corrected to eliminate all negative values. Yellow shading indicates cross-over of DPHI and NPHI which reflects gas. BVW refers to bulk volume of water and the red and blue indicates the amount of gas and water filling the pore space (%) respectively. Two shoaling upwards parasequences (Red arrows) are interpreted in the Newburg and underlying McKenzie formations. **c.** Pickett plot (left) shows water saturation (%) within the Newburg. Resistivity, PHIA and GR are plotted with respect to depth (right).

Petra™ Software was used to depth register the necessary raster logs, digitize the interval of interest, and construct cross sections and maps. Three cross sections were constructed through the study area to establish preliminary regional correlations (Figure 4.3).

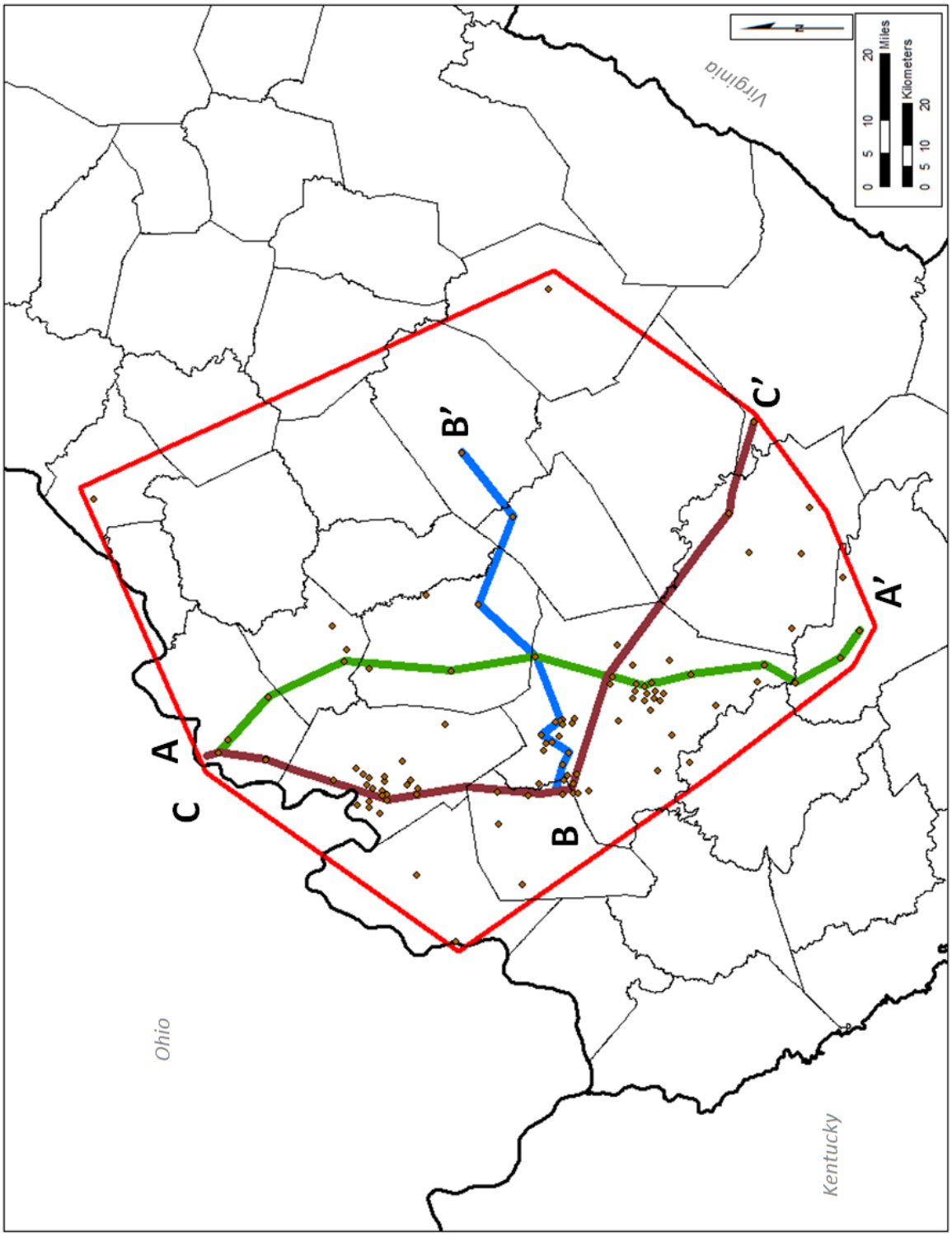
N
0 5 10 20 Miles
0 5 10 20 Kilometers
Virginia
A
A'
B
B'
C
C'
Ohio
Kentucky

Figure 4.3a


A'
B'
C'
A
B
C
20ft
4700702236
4701502644
4708704261
4703902433
4703902410
4703902369
4703902210
4703902196
4707901155
4702500022
4701900123
4701900241
4701900556
4703901684
4703902097
4707901155
4707901178
4703501196
4703501382
4703501246
4710701631
4710701266

Figure 4.3b

Figure 4.3 a. Location of regional cross-sections within the study area. **b.** Stratigraphic cross-sections using GR logs through study area. Tie wells are color coded. Color shading is indicative of gamma-ray value with lower gamma-ray values (clean sandstone and carbonate) in yellow and higher gamma-ray values (shale rich interval) gray. Datum is base of the Newburg.

Once initial correlations were completed, the Newburg in the remaining wells throughout the study area became much easier to identify. The depth map shows that, throughout the study area, the formation sits well below the 2600 ft depth limit necessary to keep CO_2 in its supercritical phase at hydrostatic conditions (Figure 4.4). The sub-sea structure shows a relatively uniform deepening to the north-east (Figure 4.5). In south-east Wirt County and central Fayette County, there appears to be an anomaly in the structure and isopach maps (Figure 4.5, 4.6). In Fayette County, thickening appears to be depositional (Figure 4.7). In Wirt County, the log signature appears to show that the section is repeated, suggesting the presence of a compressional fault (Figure 4.8). This is a previously unrecognized compressional fault cutting the Silurian and appears to be related to the Burning Springs anticline.

The average porosity map was created by digitizing the NPHI and DPHI curves (Figure 4.9). Once digitized, negative values were converted to “0” and then an arithmetic average porosity (PHIA) was calculated over the entire interval using the following equation:

PHIA = (DPHI + NPHI) / 2 (2)

Although the major Newburg gas fields are described as structural and stratigraphic traps separated by saltwater contacts (Patchen, 1996), the highest average porosities are outside of these areas which indicates that production is predominantly controlled by permeability boundaries. High porosity zones exist within the Newburg Sandstone in gas fields, but they generally represent only a quarter to a third of the entire stratigraphic interval. A pore-foot map was constructed to help identify areas with the combination of thick, high porosity in the Newburg Sandstone (Figure 4.10).

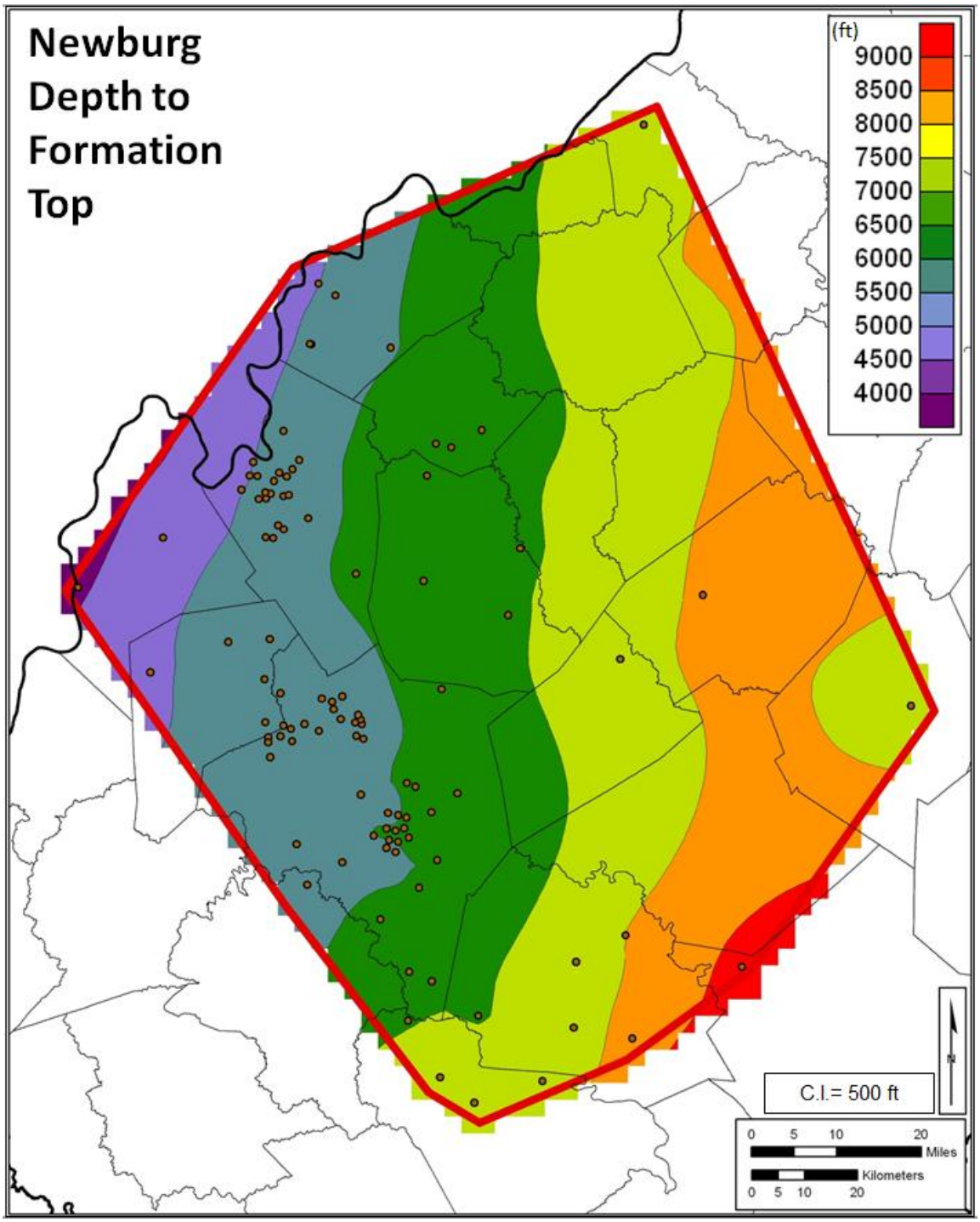

Figure 4.4 Newburg depth to formation top map. The formation lies well below the 2600 feet (800m) depth limit required to maintain and efficiently store CO_2 in a supercritical phase at hydrostatic conditions. Contour interval is 500ft (150m).

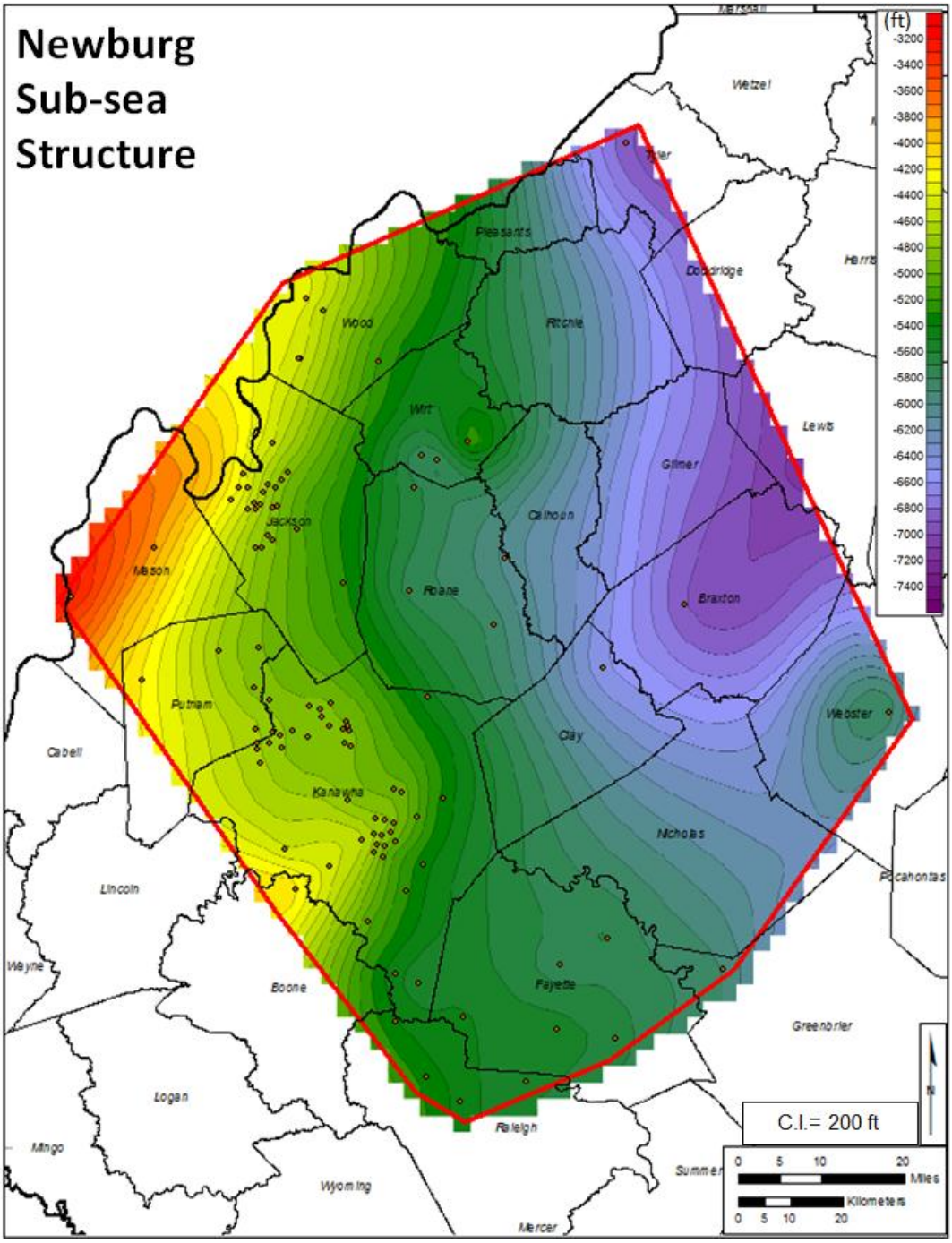

Figure 4.5 Newburg sub-sea structure map shows a relatively uniform dip to the north and north-east in the deeper parts of the foreland basin in Braxton County, West Virginia. Anomaly in Wirt County is interpreted as compressional basement faulting associated with Burning Springs anticline. Contour interval is 200ft (60m).

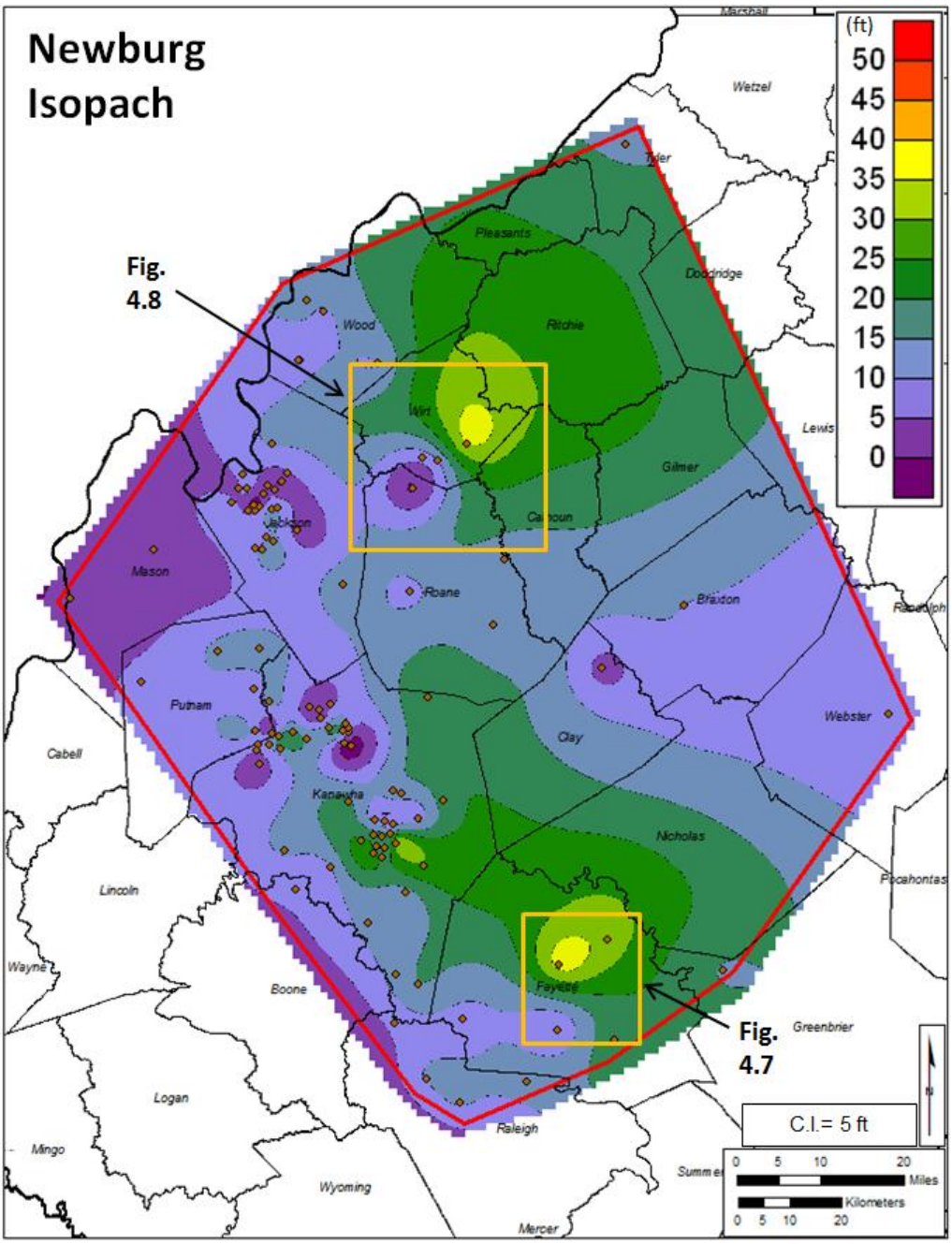

Figure 4.6 Newburg isopach map. Anomaly in Wirt County is possibly associated with basement faulting. Thin zone running east-west across central part of study area appears to coincide with an increase in average porosity across the Newburg. Contour interval is 5 ft (1.5m). Locations of Figure 4.7 and 4.8 referring to anomalous thickening events.

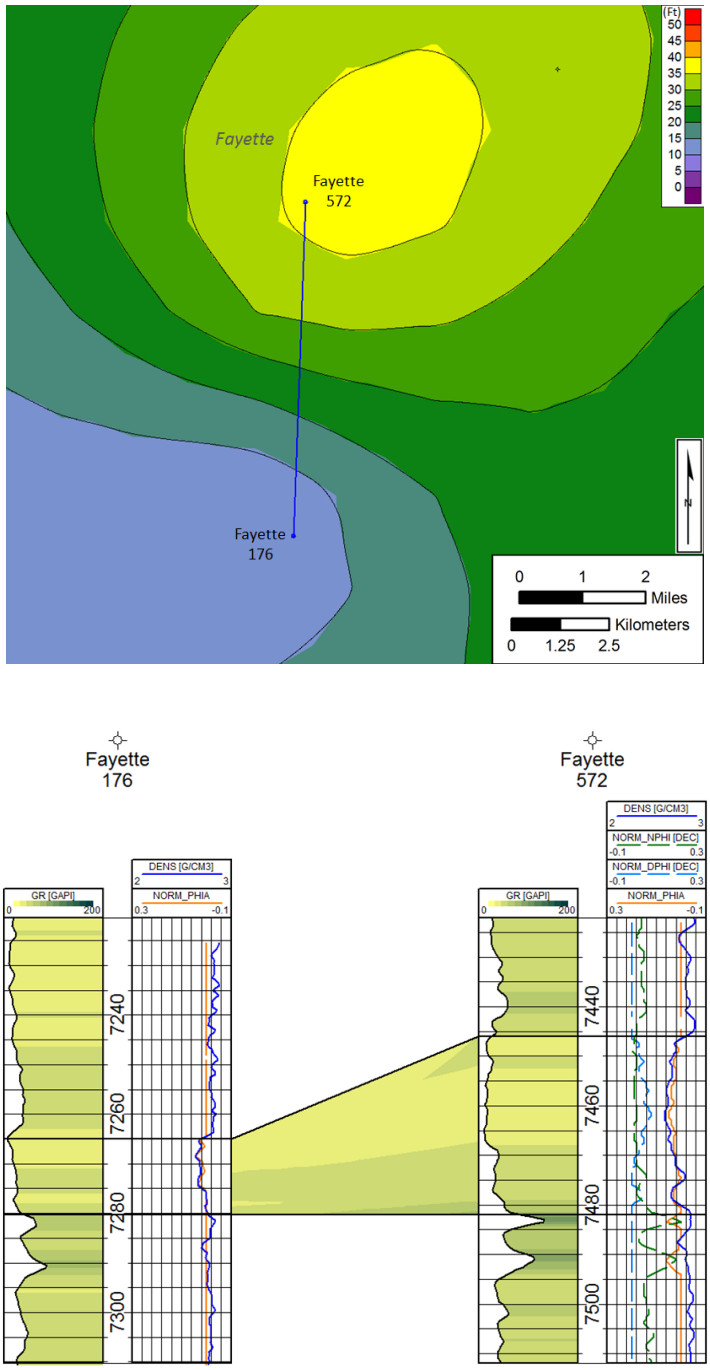

Figure 4.7 Isopach map and cross-section showing anomalous thickening of Newburg in Fayette County. This is interpreted to be a result of increased deposition of individual units.

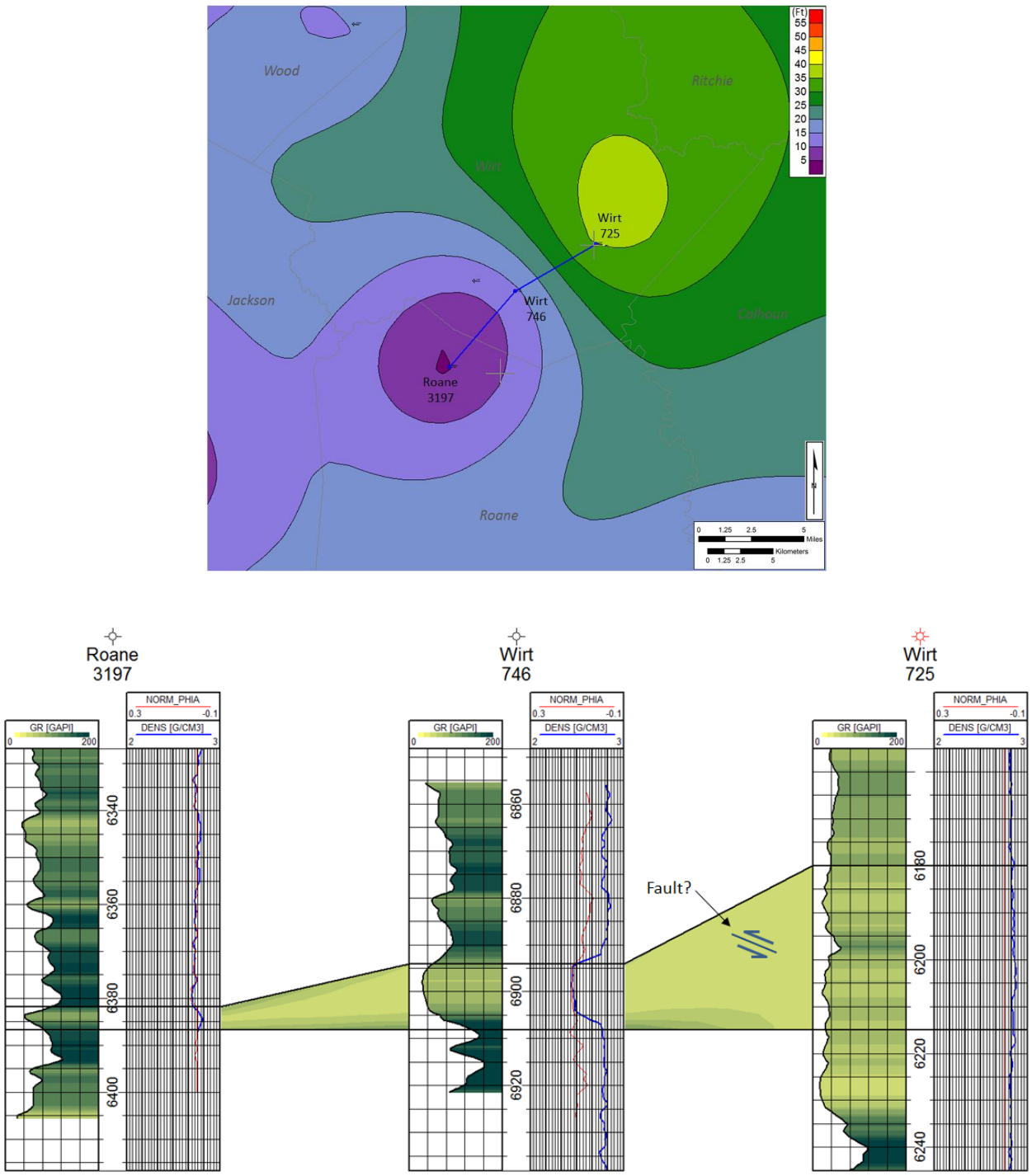

Figure 4.8 Isopach map and cross-section showing anomalous thickening of Newburg in Wirt County. GR log signature in Wirt 725 appears to repeat, which is interpreted to be a result of compressional faulting.

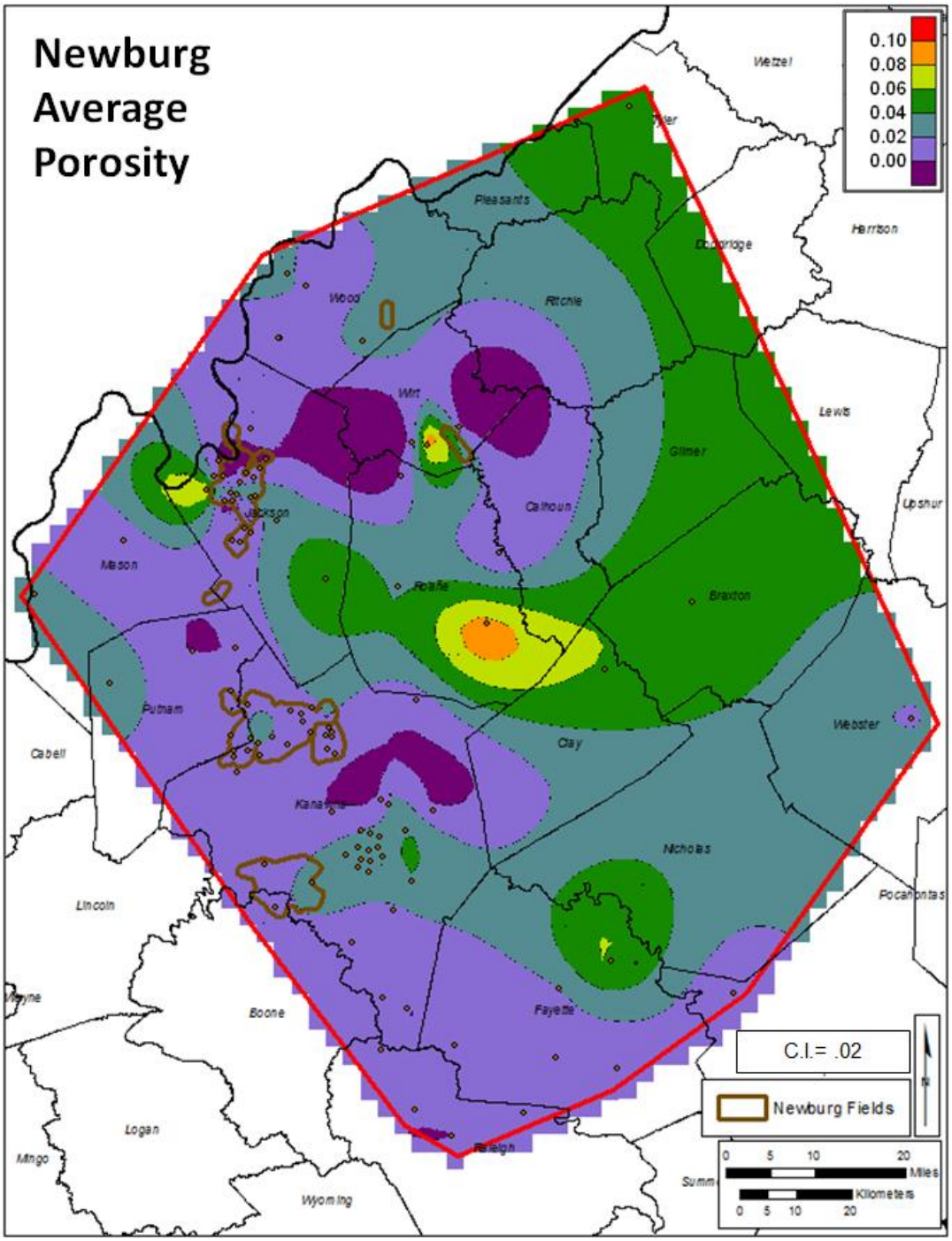

Figure 4.9 Newburg average formation porosity map. The increased average porosity zone that runs east-west across the central part of study area appears to be consistent with thinning in the Newburg. Contour interval is .02 porosity units on a scale from 0 - 1.

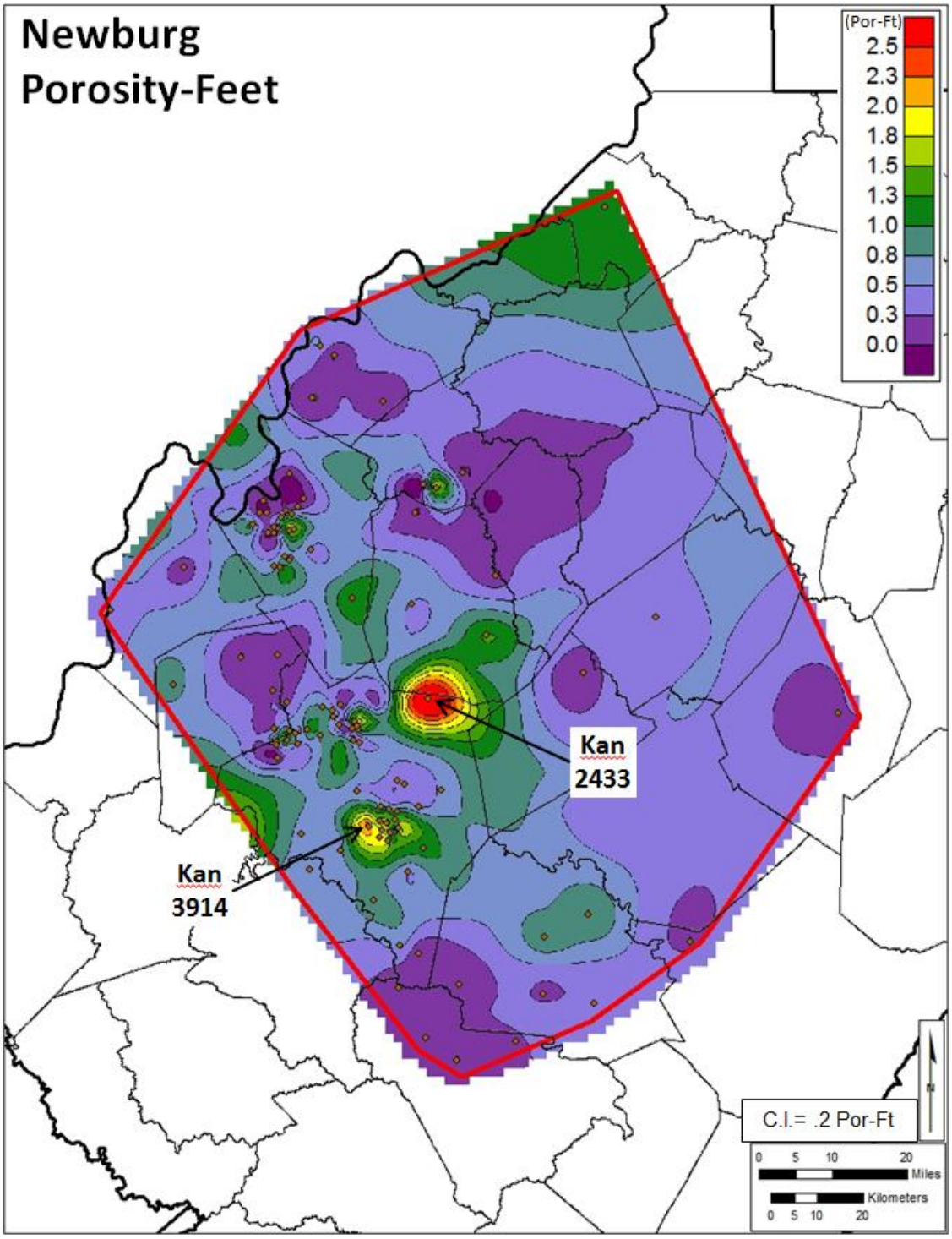

Figure 4.10 Newburg pore-foot map is used to identify the thickest zones in the study area with the highest amount of porosity. Contour interval is .2 por-ft.

The highest pore-foot areas appear to be isolated features and center around two individual wells in Kanawha County. The first, API# 4703902433, was a non-productive well that targeted the lower Silurian Tuscarora Sandstone. Although the log shows the Newburg to be very clean and porous in this well, according to well records, it is also saturated with saltwater (WVGES database, accessed July 17, 2012) (Figure 4.11).

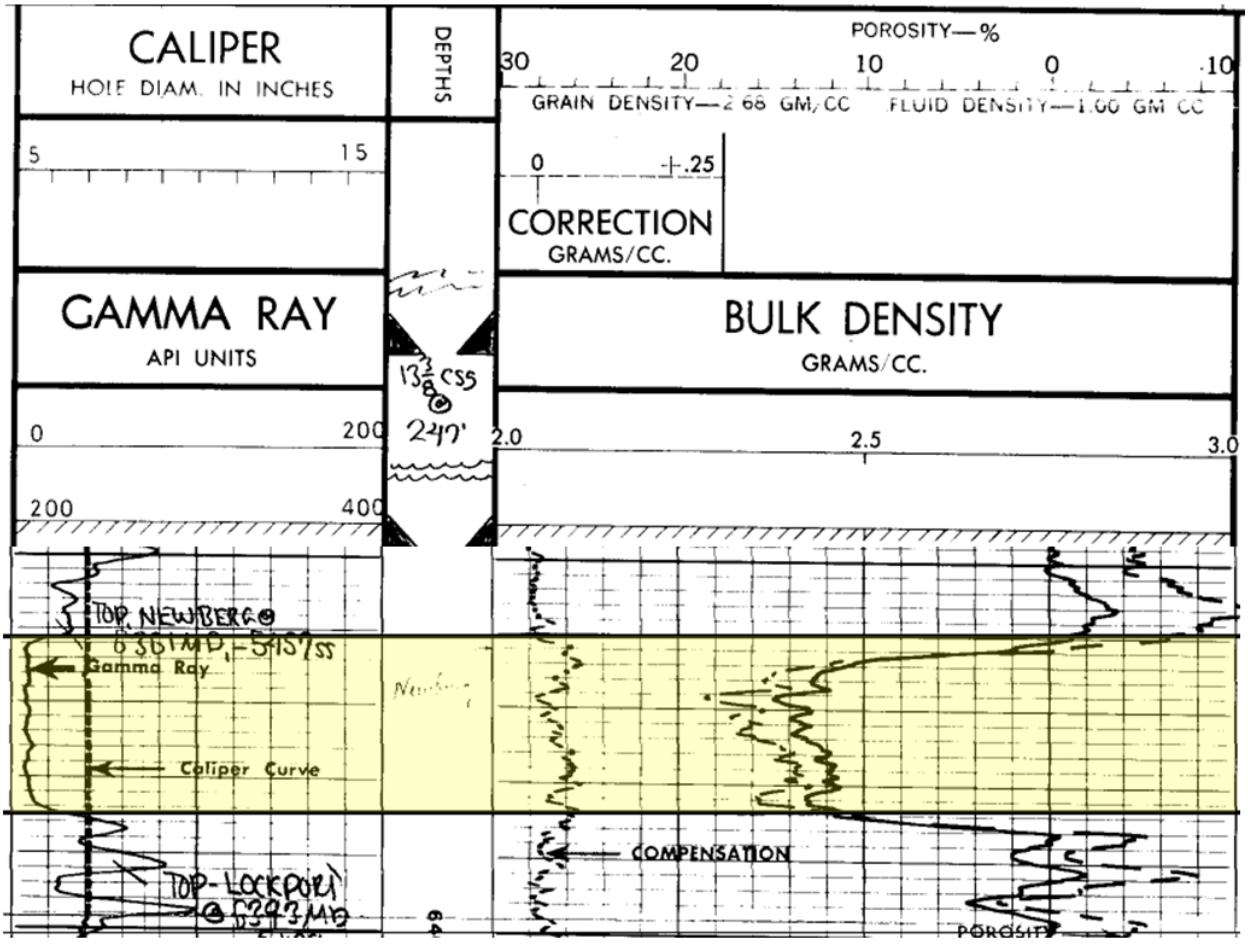

Figure 4.11 Kan 2433 (API # 4703902433). Well with highest pore-foot value for the Newburg in the study area. Salt water was produced from the Newburg in this area.

The well with the second highest pore-foot value in the study area is also located in Kanawha County. API# 4703903914 was a successful well that produced from the Tuscarora. This log has the characteristic NPHI/DPHI cross-over in the upper section of the Newburg, as well as two smaller instances in the middle and lower part of the section, indicative of gas (Figure 4.12).

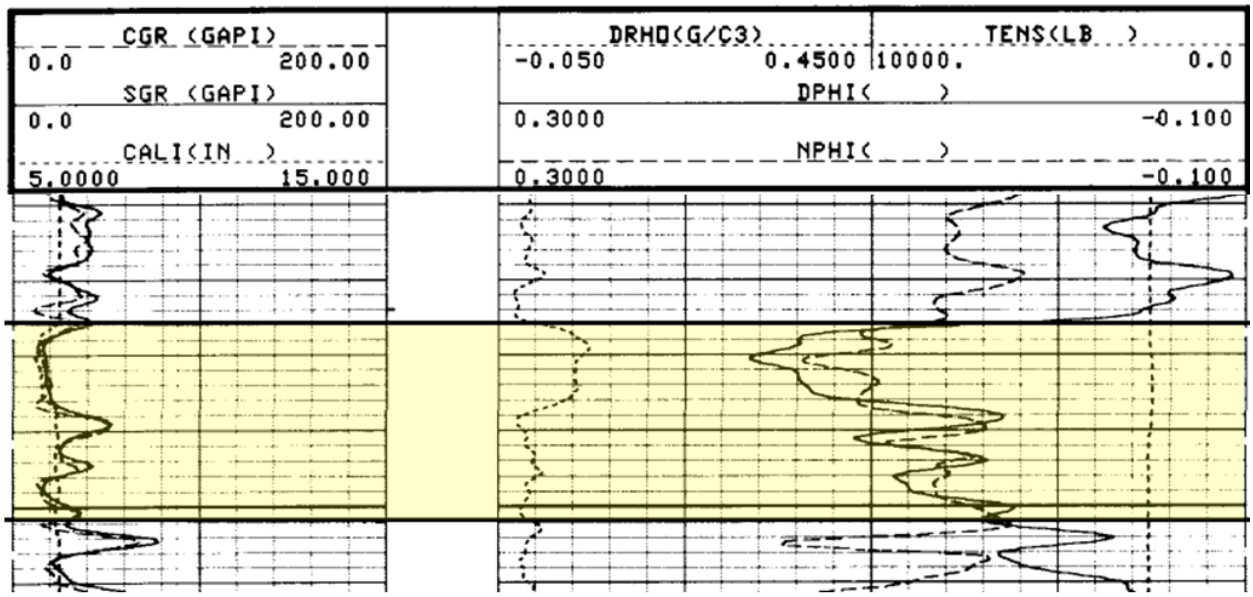

Figure 4.12 Kan 3914 (API# 4703903914). Well with second highest pore-foot value through the Newburg in the study area.

While the pore-foot map shows areas of isolated porosity, it does little to demonstrate connectivity between and across the study area. A cross-section through Jackson and Kanawha counties shows that porosities greater than or equal to 10% exist in the upper part of the Newburg section across a large area (Figure 4.13 a, b). Unfortunately, few porosity logs are available and definition of these high porosity areas is limited to the

individual producing fields. It is difficult to determine the characteristics of the formation without more well control outside of the major production fields or a better understanding of the depositional model.

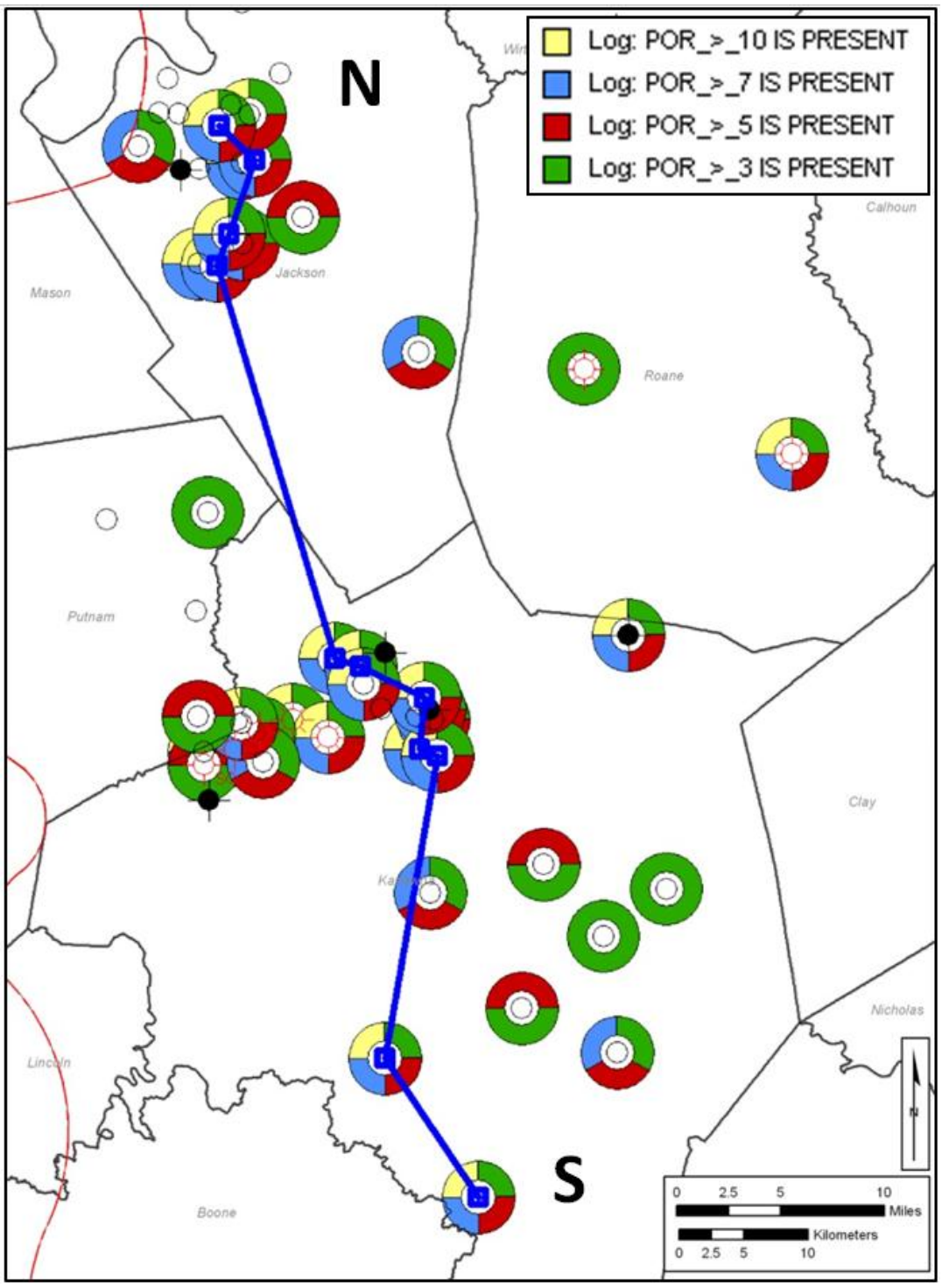
Log: POR_>_10 IS PRESENT
Log: POR_>_7 IS PRESENT
Log: POR_>_5 IS PRESENT
Log: POR_>_3 IS PRESENT
N
S
Jackson
Mason
Calhoun
Roane
Putnam
Clay
Nicholas
Lincoln
Boone
0 2.5 5 10
Miles
Kilometers
0 2.5 5 10

Figure 4.13a

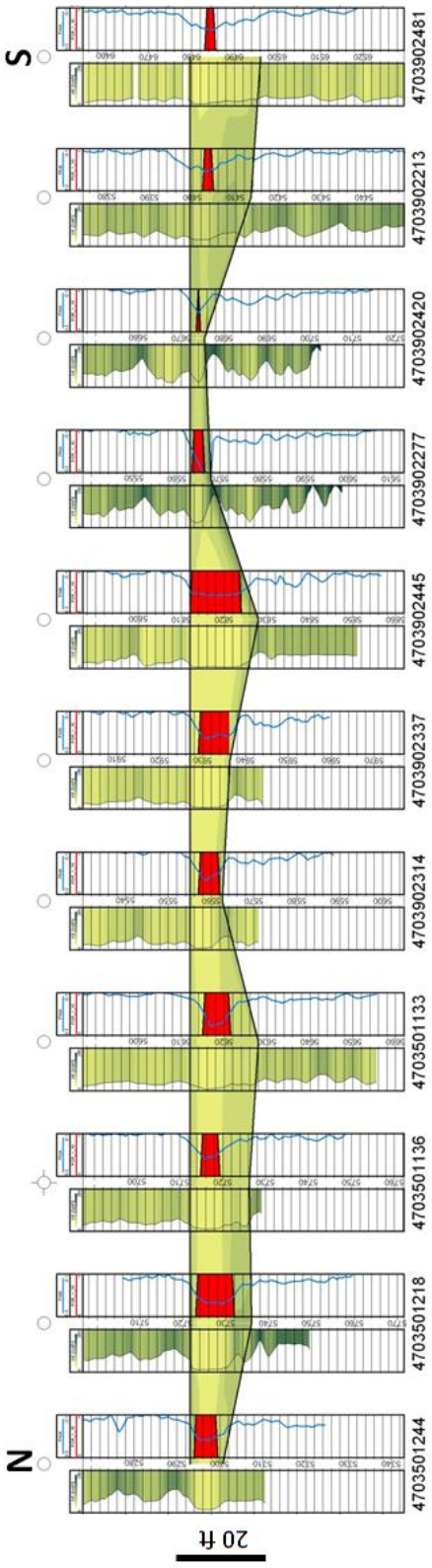
S
N
4703902481
4703902213
4703902420
4703902277
4703902445
4703902337
4703902314
4703501133
4703501136
4703501218
4703501244
20 ft

Figure 4.13b

Figure 4.13 a. Map showing locations of cross-section through Jackson and Kanawha Counties highlighting wells with Newburg porosity greater than or equal to 10%. **b.** Cross-section; datum is the top of the Newburg with porosity greater than 10% highlighted in red.

4.1 CALCULATIONS

The density of CO_2 was determined using standards set by the National Institute of Standards and Technology (NIST, 2011). Average formation temperature of the Newburg has been determined to be 130 degrees Fahrenheit (Patchen, 1996). Minimum and maximum pressures were determined by multiplying the hydrostatic gradient (0.433 pounds per square inch per foot) by the depth range of the Newburg, which is between 4,000 feet (1,220 m) and 9,000 feet (2,740 m) (Figure 4.14).

Referring to Equation (1) where:

A = 200 billion ft^2

$\mathbf{h_g}$ = 15.2 ft

$\boldsymbol{\phi_{tot}}$ = .018

$\boldsymbol{\rho}$ = 31.75 – 51.89 lbs/ft^3

E = .0051, .020, .055

The Newburg CO_2 storage potential at minimum pressure conditions of 1,732 pounds per square inch (psi) is between 4.0 and 43.4 million tonnes. The Newburg CO_2 storage potential at maximum pressure conditions of 3,897 pounds per square inch (psi) is between 6.6 and 71.0 million tonnes (Figure 4.14). Annual CO_2 emissions in West Virginia is approximately 77 million tonnes (NATCARB, 2012); therefore, the potential storage capacity for the Newburg is less than one year of West Virginia's emissions.

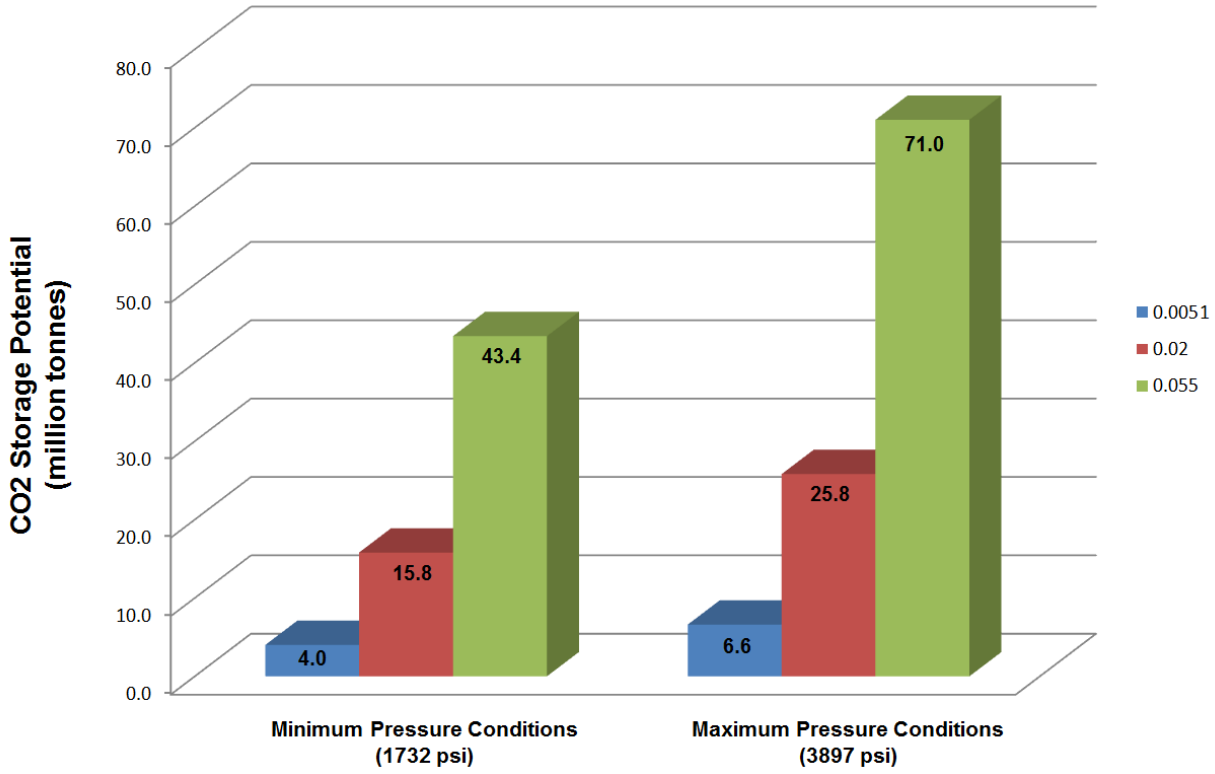

Figure 4.14 Newburg CO_2 storage potential at maximum and minimum pressure conditions.

5.0 REFINING THE DEPOSITIONAL MODEL

Coring in the Newburg fields was difficult due to lack of cement in the pay zone (Patchen, 1996). Two wells (API#'s 4707901155, 4710701266) had the necessary log suites for a detailed analysis. In addition, four cored wells (API#'s 4708700714, 4703902112, 47032501136 and 4703501224,) allowed for a detailed description from the base of the Salina, through the Newburg, into the top of the McKenzie. Several samples were taken from these cores and used to make thin sections illustrating typical and unusual features (Figure 5.1).

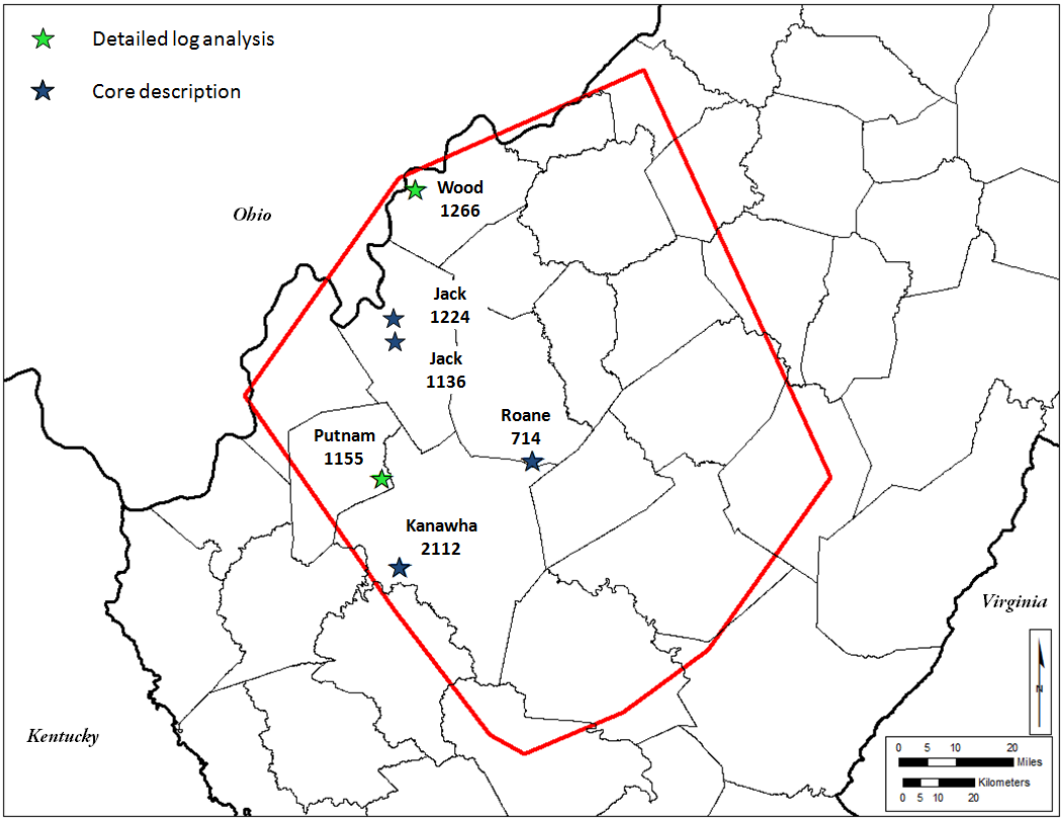

Figure 5.1 Study area with locations of wells with detailed log analysis and core descriptions.

5.1 Core Analysis

Core from the Roane 714 (API# 4708700714) well starts in the Newburg at a depth of 6,284 ft (1,915 m) and continues into the McKenzie to a depth of 6,299 ft (1,920 m). This well is located in the center of the study area and was originally drilled as an unsuccessful test of the Tuscarora Sandstone. Spudded in 1957, the well's gamma ray trace is recorded in micrograms RA EQ per ton units while the Neutron is in standard counts per second (Figure 5.2 a.). The core is a mix of fine-grained silty/sandy carbonate and fine-grained sandstone. A common feature throughout the core is clay beds that have been disrupted by various degrees of bioturbation. A dark-grey shale interval exists at 6,290 ft (1,917 m). This shale is picked on the log as a spike in the gamma ray count and is interpreted as the top of the McKenzie Formation, making the core about two feet shallower than the log. Immediately below this shale is a silica-cemented, fine-grained quartz sand with vugs, shale clasts and signs of bioturbation. Above the shale interval, ostracodes are visible in the core (Figure 5.2 b and c).

Several thin sections were taken from the Newburg in this core. They show poorly sorted, sub-angular quartz grains isolated in a clay-rich and carbonate matrix. In thin section, dolomite rhombs appear sporadically throughout the interval and microfossils (possibly ostracodes) are present at the top of the core (Figure 5.2 d). Carbonate cement occurs filling intergranular and fracture porosity (Figure 5.2 d, e). Minimal porosity still exists, as dissolution of sediments is evident (Figure 5.2 d). The distribution of the clay particles among the quartz grains in Figure 5.2 d appears to be

uneven. This may be due to bioturbation if the area of calcite cement is interpreted as a burrow, where this uneven distribution is especially noticeable (Figure 5.2 d).

In the upper part of the McKenzie, storm deposits, indicated by intraclasts, are generally followed by a gradual return to biological activity. The two shale layers are interpreted as rises in sea level, which subsequently fell, allowing for a slow restoration of biologic activity (Figure 5.2 c.). Faunal content increases towards the top of Newburg; however, the gamma ray increase that overlies the Newburg suggests one last rise in sea level before deposition of the Salina evaporite sequence (Figure 5.2 a.). Circulation and wave action appear to be intermittent, thus creating an environment subjected to rapid changes in localized sea level, perhaps in a tidal channel. The repetitive nature of these deposits is noticeable in the core and on the GR curve through the Newburg in this well and is interpreted as being part of a set of marine parasequences, reflecting a prograding shoreline (Figure 5.2a.) These sequences are recognized by a series of coarsening upward successions separated by a flooding surface, typically represented by shale deposits (Kamola and Wagoner, 1995).

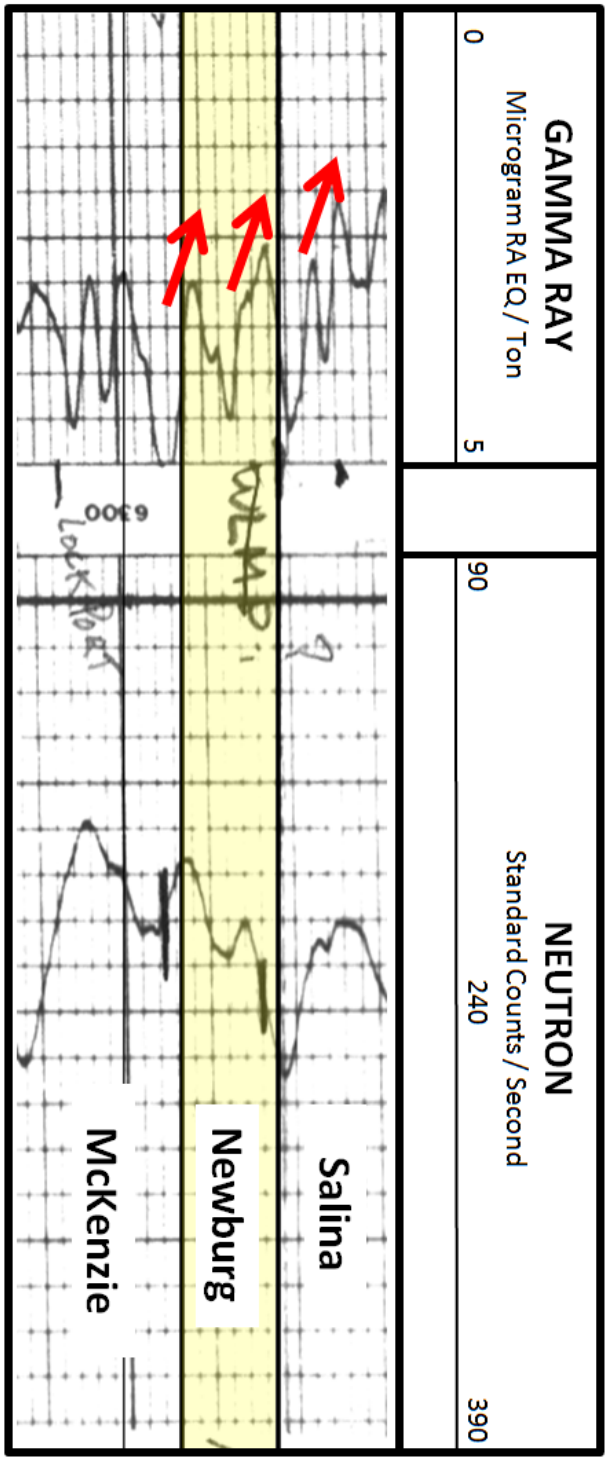
GAMMA RAY
Microgram RA EQ / Ton
0
5
NEUTRON
Standard Counts / Second
90
240
390
Salina
Newburg
McKenzie

Figure 5.2a

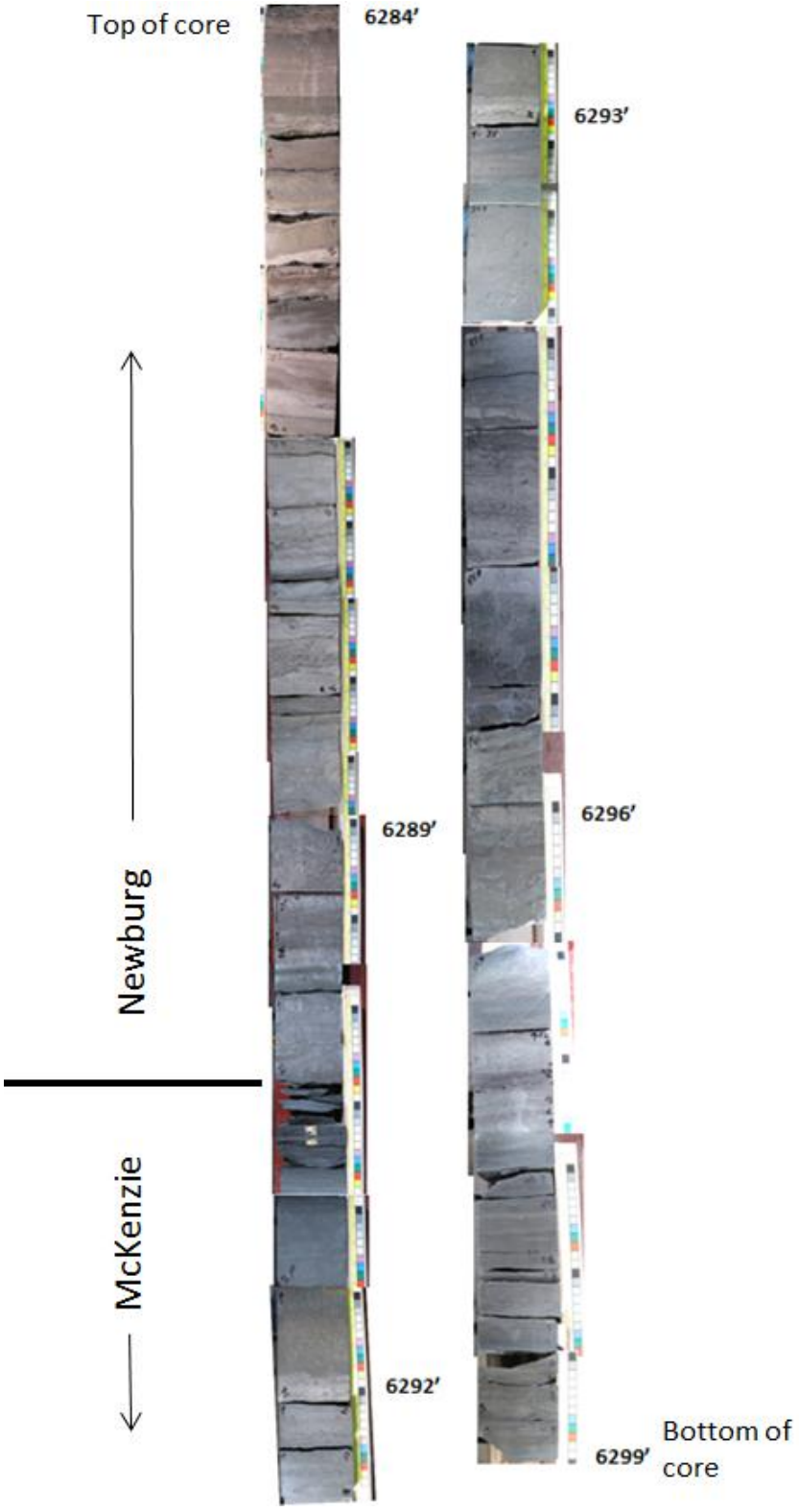
Top of core
6284'
6293'
6289'
6296'
Newburg
McKenzie
6292'
6299'
Bottom of core

Figure 5.2b

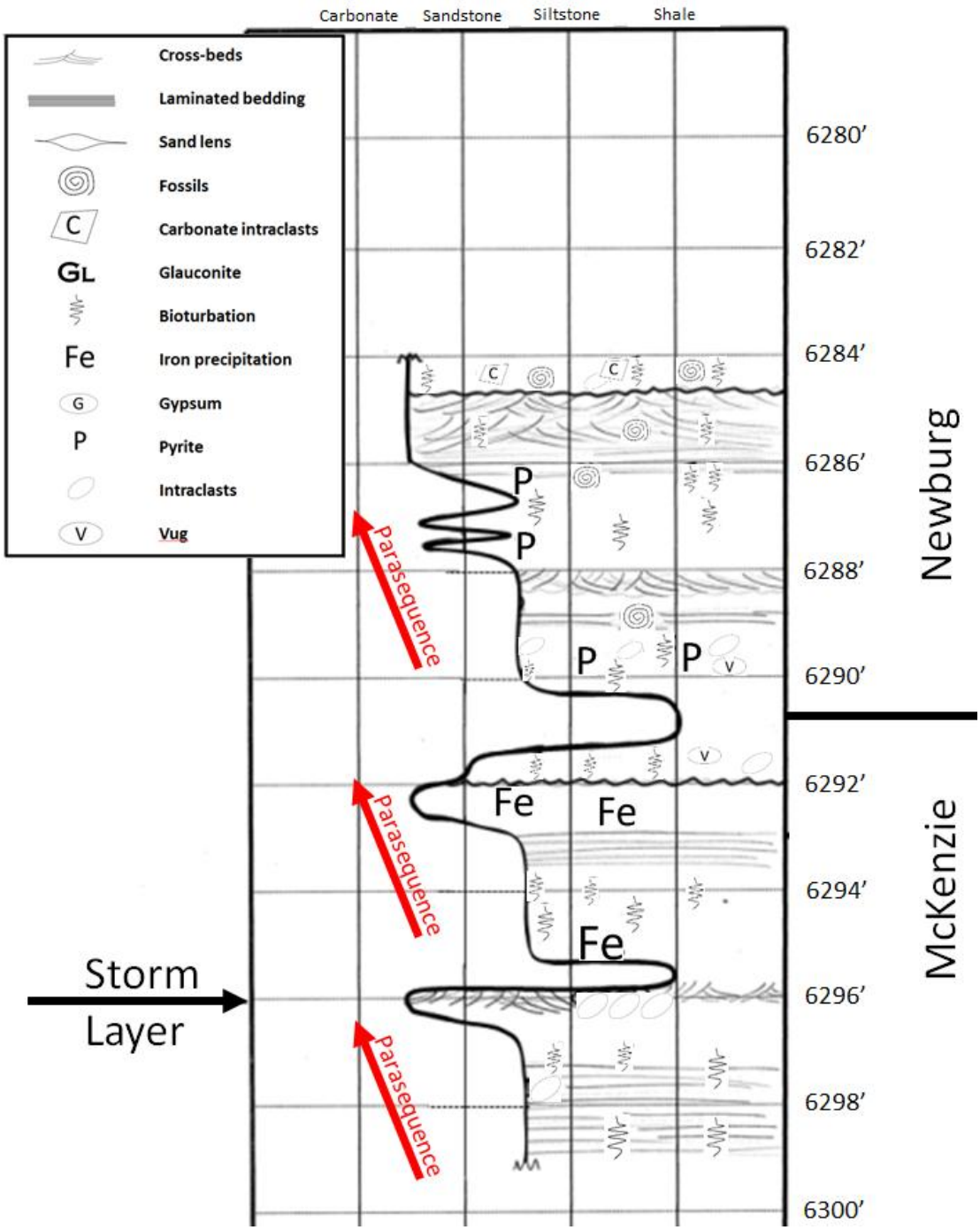
Carbonate
Sandstone
Siltstone
Shale
Cross-beds
Laminated bedding
Sand lens
Fossils
C
Carbonate intraclasts
GL
Glauconite
Bioturbation
Fe
Iron precipitation
G
Gypsum
P
Pyrite
Intraclasts
V
Vug
6280'
6282'
6284'
6286'
6288'
6290'
6292'
6294'
6296'
6298'
6300'
Newburg
McKenzie
Parasequence
Parasequence
Parasequence
Storm
Layer
P
P
P
P
Fe
Fe
Fe
C
C
V
V

Figure 5.2c

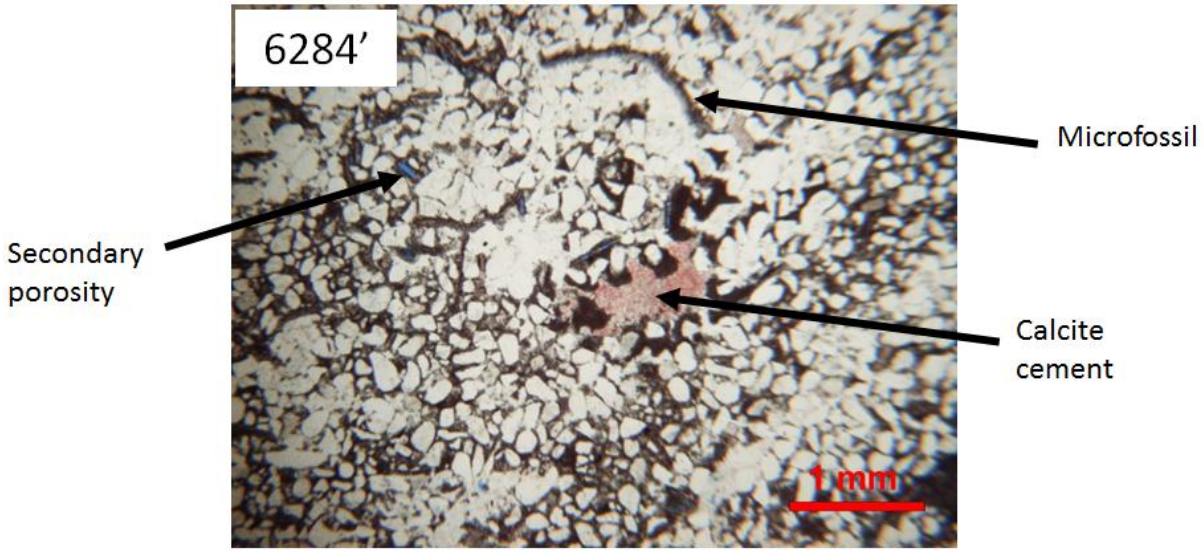

Figure 5.2d

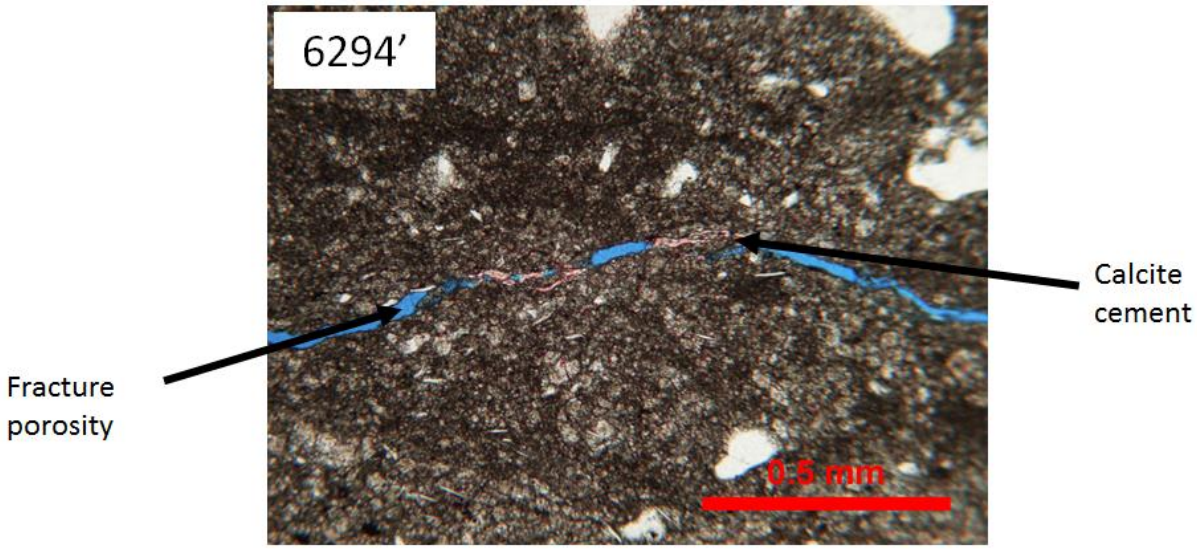

Figure 5.2e

Figure 5.2 Roane 714 (API# 4708700714) Geophysical log **(a.)**, photographed core **(b.)**, lithological log **(c.)** and thin sections **(d. and e.)**. Yellow color in geophysical log represents the Newburg. Blue color in thin sections represents porosity. Red arrows on logs and core description (a. and c.) indicate individual parasequences.

Core from the Kanawha 2112 (API# 4703902112) well is taken from the Kanawha Forest field; however, no production is documented from this well. The cored interval includes the base of the Salina and most of the Newburg between the depths of 5,400 and 5,432.5 ft (1,646 and 1,656 m) (Figure 5.3 a). Completed in 1967, the well was fractured in the Newburg and labeled as a development. The targeted production depth, 5418-5430 ft (1,651- 1,655 m), is marked at the top by an anomalous decrease in bulk density that coincides with a porosity increase. The log shows fluctuations in the gamma ray count in the transition from the McKenzie to the Newburg. The high gamma ray count towards the bottom of the Newburg is interpreted as a shale zone (Figure 5.3 a).

This core is predominantly composed of sandy carbonate with bioturbation throughout and is difficult to correlate with the log due to the lack of available continuous core. If one uses the black carbonaceous shale in the core at 5416 ft (1651 m) as the base of the Salina, picked as high gamma ray values on the log and the “transitional zone” at 5424 ft (1653 m) as the most porous value on the log, the core appears to be four to five feet shallower than the log. It is in this “transitional zone” where dramatic changes in oxygen content occurred, indicated not only by color, but also by variations in the level of biological activity which are evidenced by fossil voids and bioturbation. Algal laminae, disrupted by bioturbation and underlain by poorly cemented red and green layers; indicating either an abrupt transition from oxygen rich to anoxic conditions or a change in salinity or weather conditions. Overlying the transitional zone, where biologic activity appears to become more intermittent, the transition from the Newburg to the

Salina is picked at a depth of approximately 5,418 ft (1,651 m) where core is missing (Figure 5.3 c). Up-section in the Salina, at core depths of 5,406 ft and 5,411 ft (1,648 and 1,649 m), brittle, black carbonaceous shale lies between cross-beds of sandy carbonate (Figure 5.3 b). The presence of carbonaceous black shales may indicate low intertidal conditions which are more influenced by fluvial processes rather than marine, indicative of an estuarine setting (Dalrymple *et al*, 1992).

Gypsum is identified in the Salina section of the core as filling in fractures and burrows. It is also present in the "pay zone" of the Newburg as part of the matrix. A closer look at 5,426.15 ft (1,654 m) shows that the gypsum is replacing dolomite (Figure 5.3 d). Intergranular porosity exists just below this zone and in some cases appears to be a result of dolomite replacement (Figure 5.3 e).

The repetitive conditions of shale, overlain by intervals of gray silt, which transition into brown sandstone persist throughout the remaining deposition of the Newburg and into the Salina and are reminiscent of the parasequences described in the Roane 714 core.

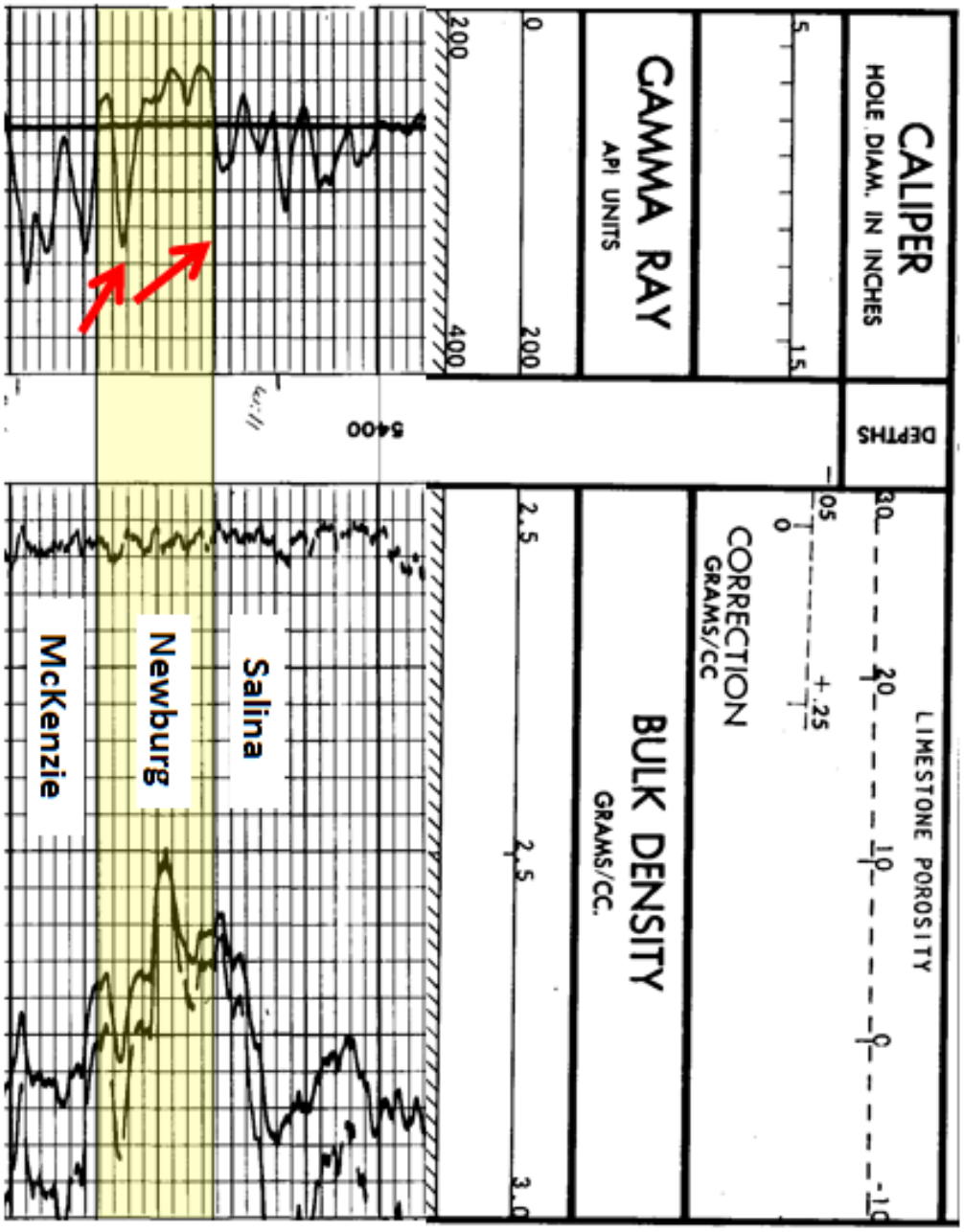
CALIPER
HOLE DIAM. IN INCHES
5
15
GAMMA RAY
API UNITS
0
200
200
400
DEPTHS
5400
LIMESTONE POROSITY
30
20
10
0
-10
CORRECTION
GRAMS/CC
.05
0
+.25
BULK DENSITY
GRAMS/CC.
2.5
2.5
3.0
Salina
Newburg
McKenzie

Figure 5.3a

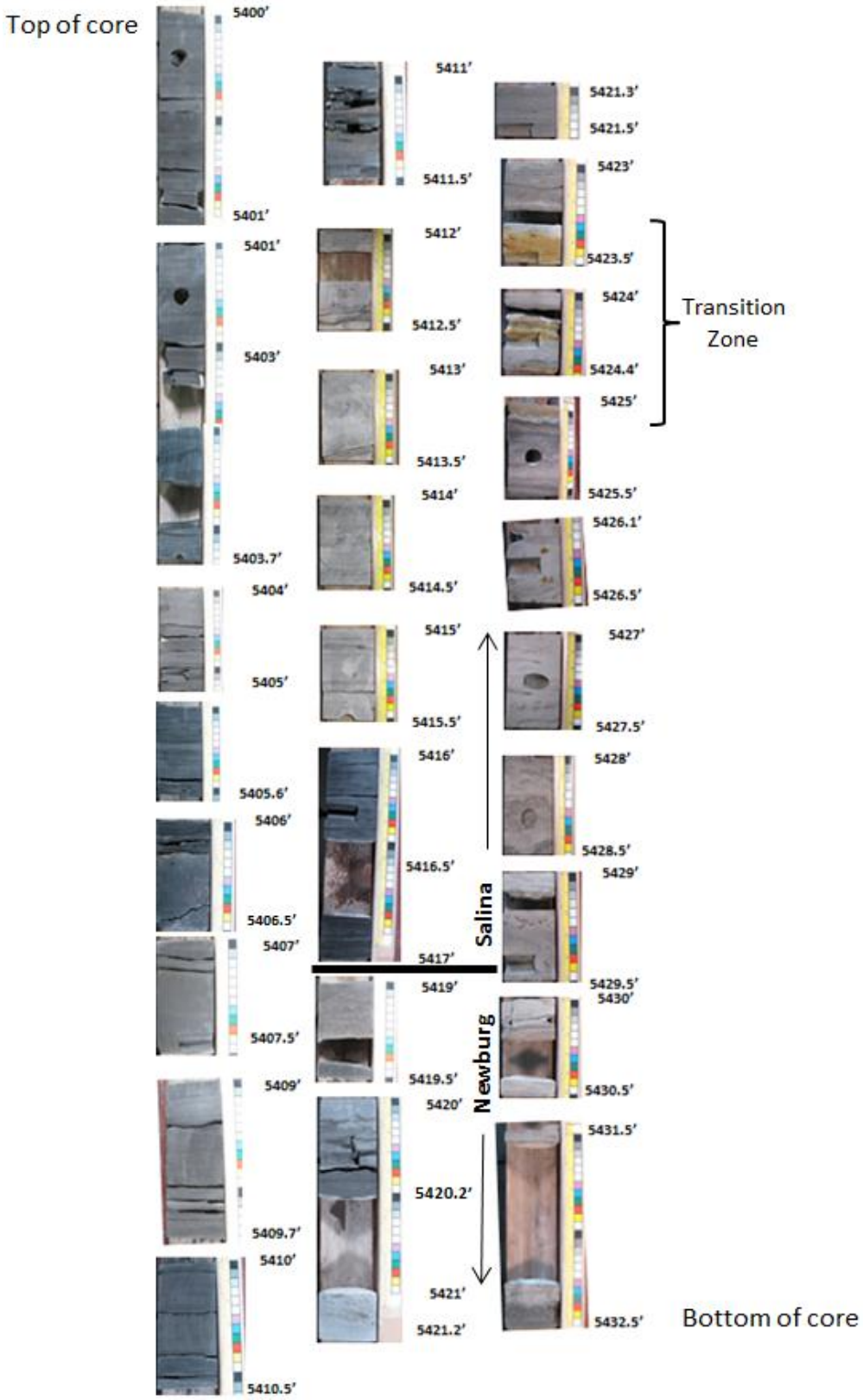
Top of core
5400'
5401'
5401'
5403'
5403.7'
5404'
5405'
5405.6'
5406'
5406.5'
5407'
5407.5'
5409'
5409.7'
5410'
5410.5'
5411'
5411.5'
5412'
5412.5'
5413'
5413.5'
5414'
5414.5'
5415'
5415.5'
5416'
5416.5'
5417'
5419'
5419.5'
5420'
5420.2'
5421'
5421.2'
5421.3'
5421.5'
5423'
5423.5'
5424'
5424.4'
5425'
5425.5'
5426.1'
5426.5'
5427'
5427.5'
5428'
5428.5'
5429'
5429.5'
5430'
5430.5'
5431.5'
5432.5'
Transition Zone
Salina
Newburg
Bottom of core

Figure 5.3b

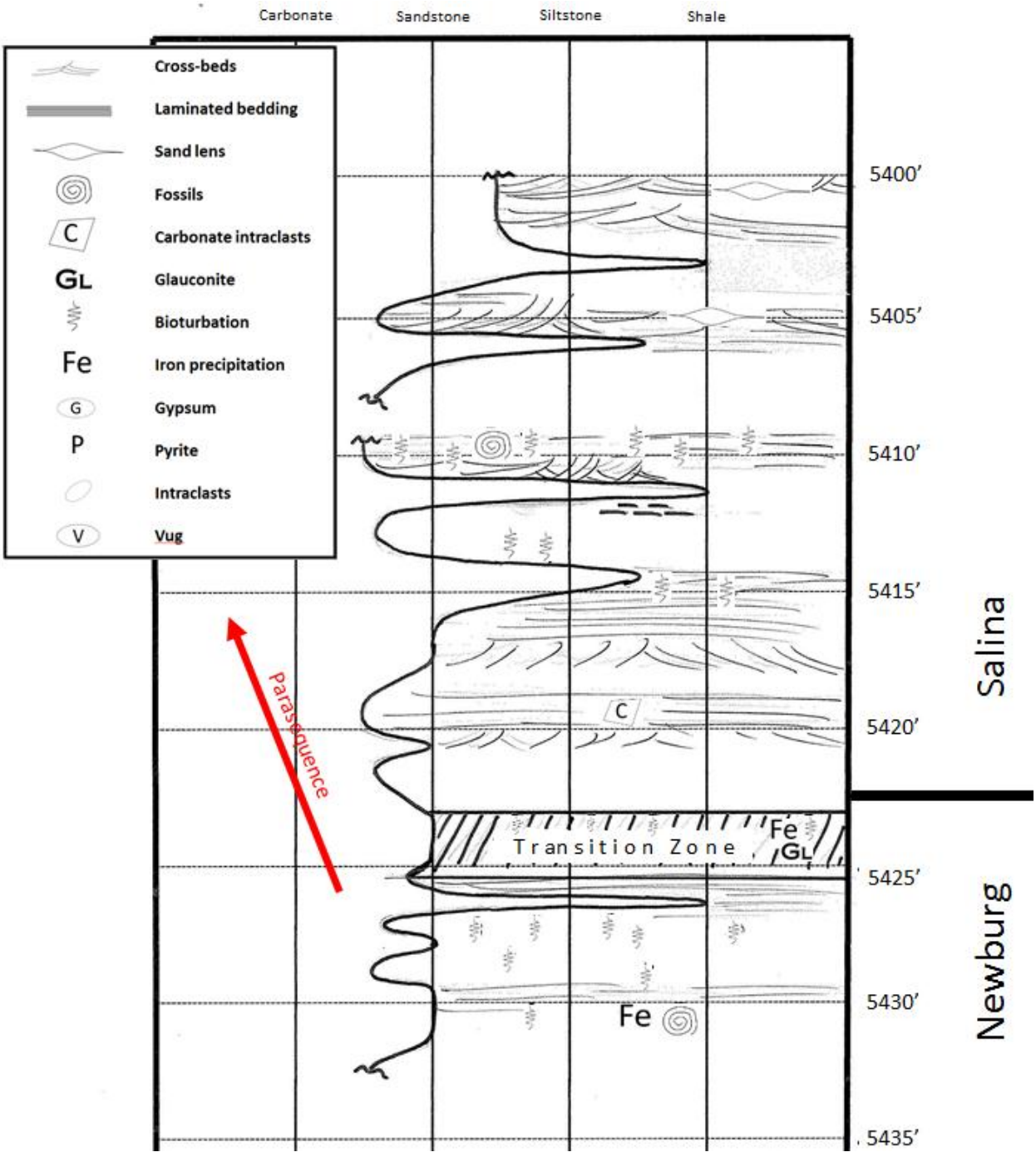
Carbonate
Sandstone
Siltstone
Shale
Cross-beds
Laminated bedding
Sand lens
Fossils
C
Carbonate intraclasts
GL
Glauconite
Bioturbation
Fe
Iron precipitation
G
Gypsum
P
Pyrite
Intraclasts
V
Vug
5400'
5405'
5410'
5415'
5420'
5425'
5430'
5435'
Salina
Newburg
Parasequence
C
Transition Zone
Fe
GL
Fe

Figure 5.3c

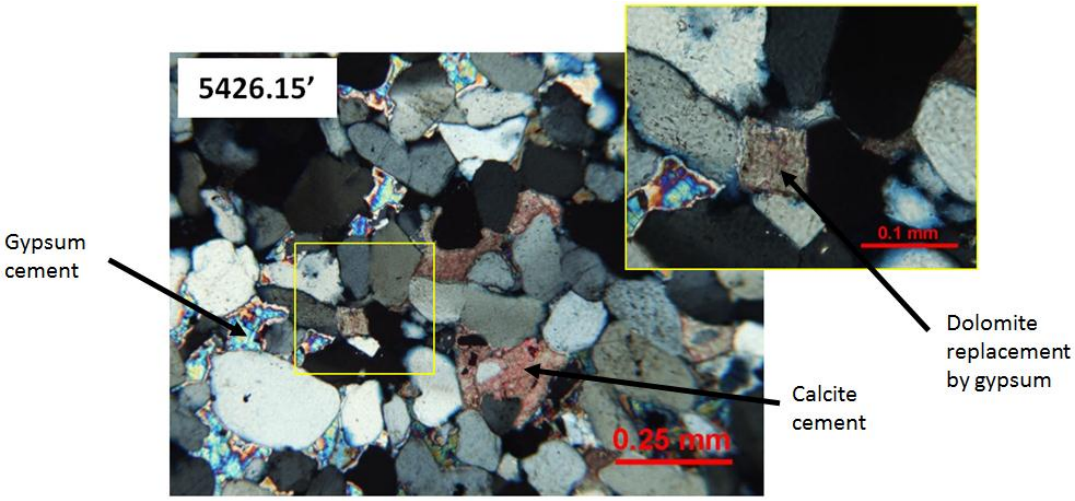

Figure 5.3d

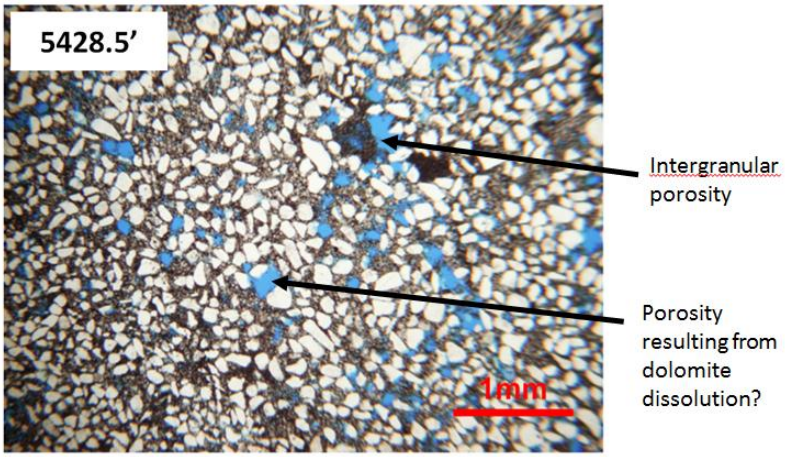

Figure 5.3e

Figure 5.3 Kanawha 2112 (API# 4703902112) Geophysical log **(a.)**, photographed core **(b.)**, lithological log **(c.)** and thin sections **(d and e.)**. Yellow color in geophysical log represents the Newburg. Blue color in thin sections represents porosity. Red arrows on logs (a. and c.) indicate individual parasequences.

The Jackson 1136 (API# 4703501136) well is located in the South Ripley Newburg field. Completed in 1967, was classified as unsuccessful. The cored interval includes the base of the Salina, and the top of the McKenzie and appears to run deeper than the log signature by about one and a half feet (Figure 5.4 a). Although the Newburg is in disarray and could not be confidently placed in stratigraphic order, one can still identify similar parasequences in the core to those previously described when compared with the log.

The base of the core consists of interbedded sands and shales suggesting abrupt changes in local environment (to a lesser scale than the “transition zones” observed in the Kanawha 2112 core). The contact between the McKenzie and the Newburg, at a core depth of 5,727.5 ft (1,746 m), appears as a change from gray silty shales with periodic intraclasts, into clean, cross-bedded, white quartz sandstone that contains some bands of organic material, or clays, and finer quartz sand layers (Figure 5.4 b). Preceded by an episode of black shale deposition at 5,730 ft (1,747 m), a regressive sequence picked at the high, “clean” gamma ray trace on the log (Figure 5.4 a).

Although it is disorganized, several pieces of core were marked with footage values in the Newburg section. A thin section at 5,715.5 ft (1,742 m) shows some calcite spar filling pore space between quartz grains (Figure 5.4 d). A closer look at this section shows gypsum filling in the pore space between the individual grains (Figure 5.4 e).

Dolomite rhombs appear to be replaced by gypsum, as they do in the Kanawha 2112 core.

The Newburg appears to begin with a low energy, tidal pool, or lagoonal deposit, which transitions into potential tidal channel deposits. Generally, the questionable section of this core appears to reinforce the shoaling upward sequence with silt intervals and shale transitioning to coarser grained sandstone as you move up section (Figure 5.4 b). The transition into the Salina shows a dramatic gamma-ray increase, normally interpreted as shale, which implies a localized rise in sea level signaling the beginning of another parasequence.

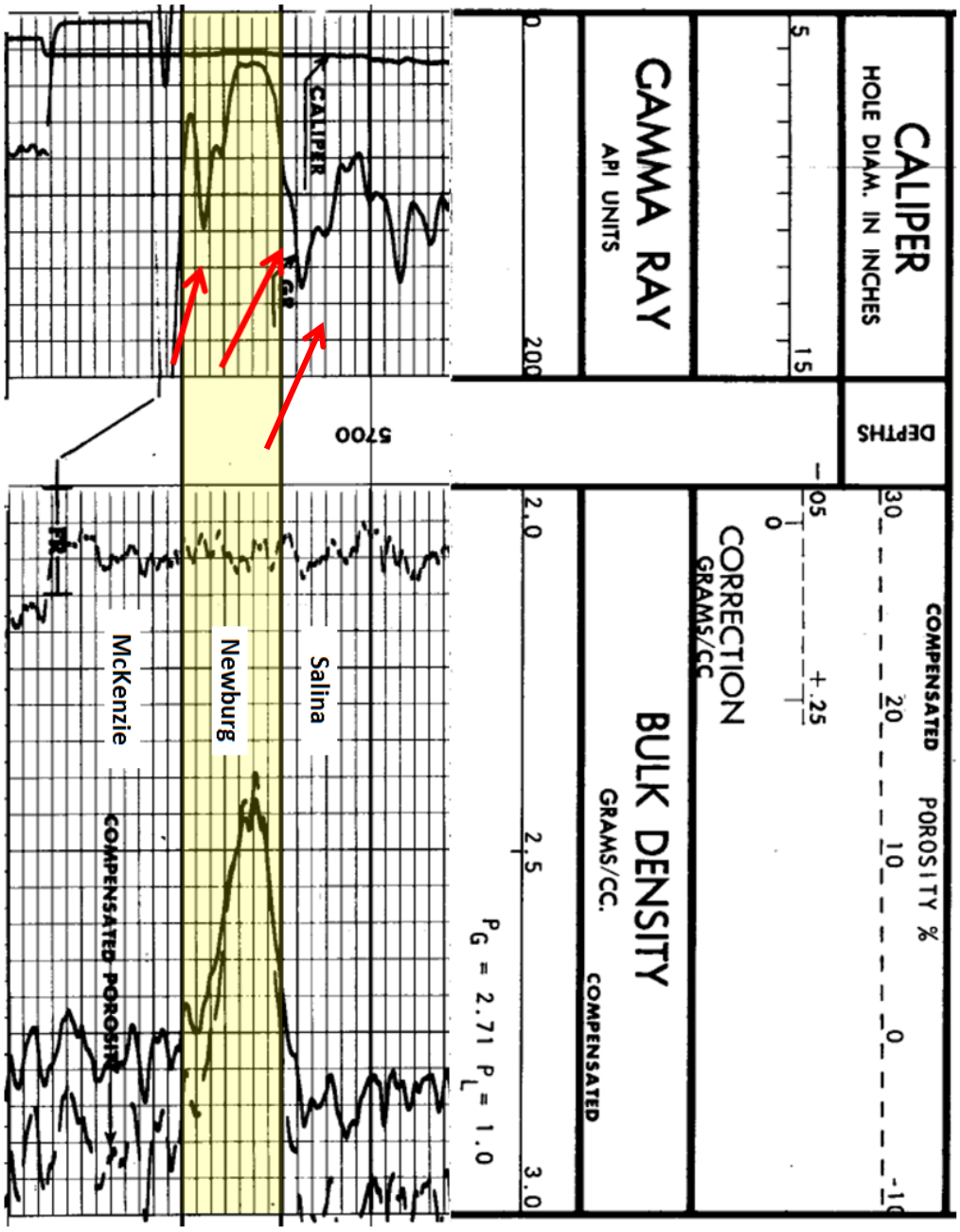
CALIPER
HOLE DIAM. IN INCHES
5
15
GAMMA RAY
API UNITS
0
200
DEPTHS
5700
COMPENSATED
POROSITY %
30
20
10
0
-10
+.25
0
CORRECTION
GRAMS/CC
BULK DENSITY
GRAMS/CC.
COMPENSATED
2.0
2.5
3.0
P_G = 2.71 P_L = 1.0
CALIPER
GR
Newburg
Salina
McKenzie
COMPENSATED POROSITY

Figure 5.4a


Top of core
5701'
5702'
5703'
5704'
5705'
5706'
5707'
Salina
5707'
5708'
5709'
5710'
Salina
5724'
5725'
5726'
5727'
McKenzie
5727'
5728'
5729'
5730'
5731'
5732'
5733'
McKenzie
Bottom of core

Figure 5.4b

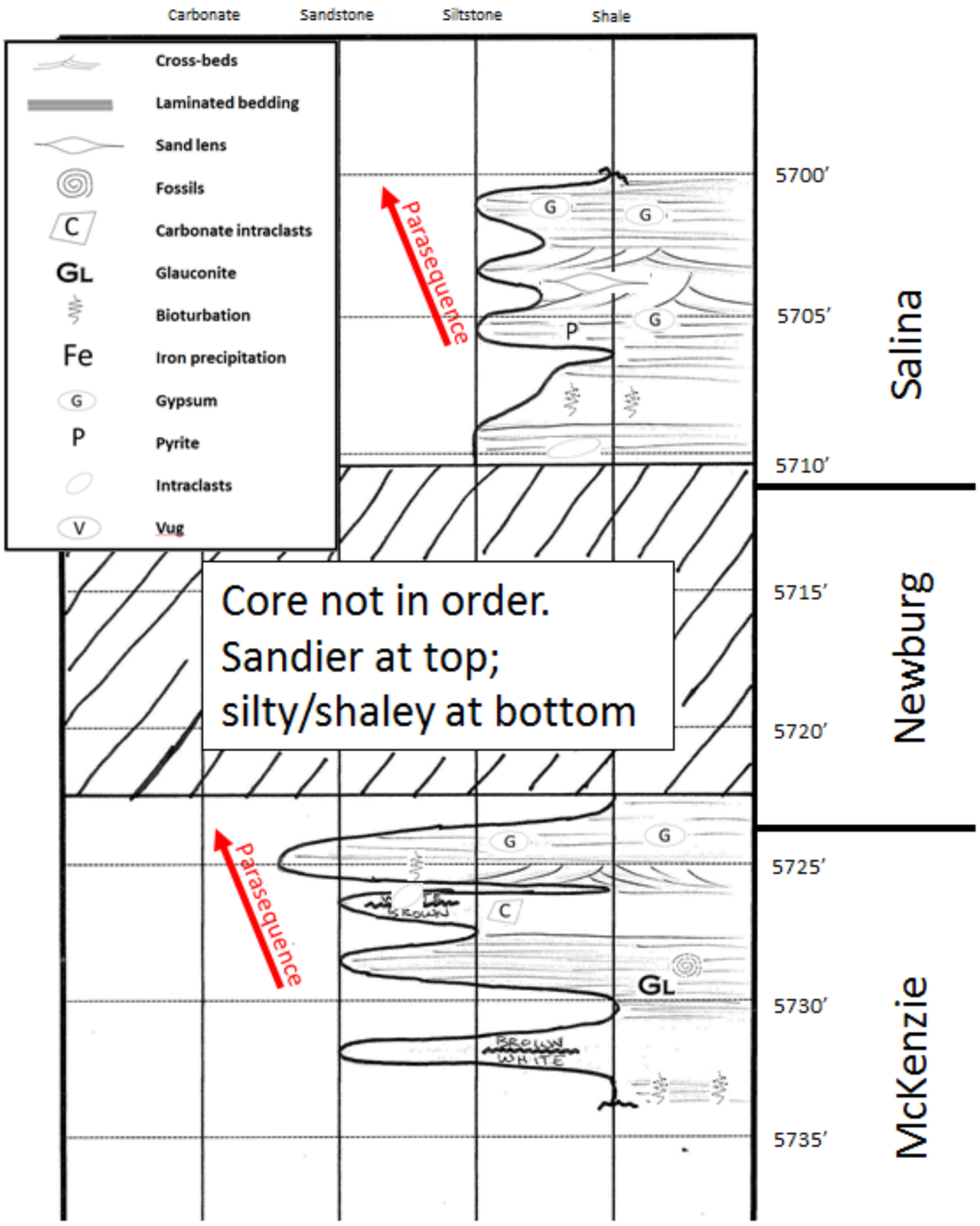
Carbonate
Sandstone
Siltstone
Shale
Cross-beds
Laminated bedding
Sand lens
Fossils
C
Carbonate intraclasts
GL
Glauconite
Bioturbation
Fe
Iron precipitation
G
Gypsum
P
Pyrite
Intraclasts
V
Vug
Parasequence
Parasequence
Core not in order.
Sandier at top;
silty/shaley at bottom
5700′
5705′
5710′
5715′
5720′
5725′
5730′
5735′
Salina
Newburg
McKenzie

Figure 5.4c

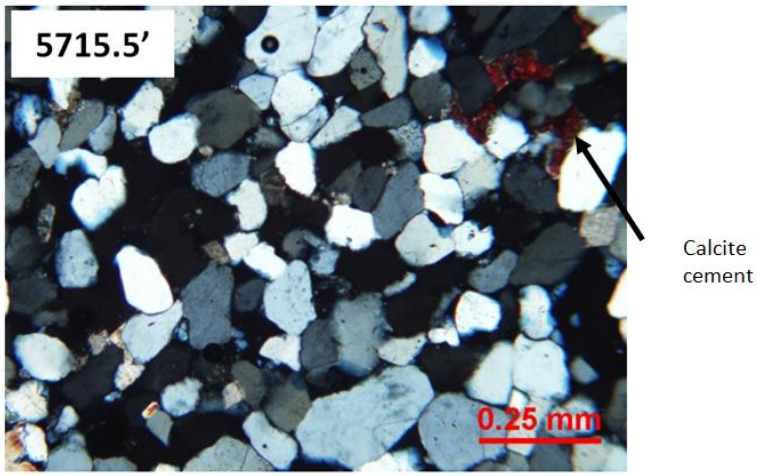

Figure 5.4d

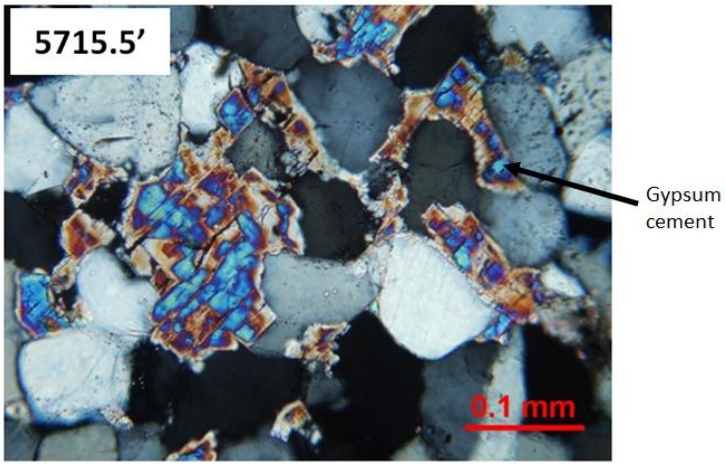

Figure 5.4e

Figure 5.4 Jackson 1136 (API# 4703501136) Geophysical log **(a.)**, photographed core **(b.)** (Red “X” indicates depth at which the core was not in order and thus, not photographed), lithological log **(c.)** and thin sections **(d. and e.)**. Yellow color in geophysical log represents the Newburg. Blue color in thin sections represents porosity. Red arrows on logs (a. and c.) indicate individual parasequences.

5.2 Log Analysis

An Excel™ spreadsheet, with macros and formulas prepared by Dr. Tim Carr (2008), was used to conduct a detailed log analysis on two wells in the study area. The curves used for these calculations include photoelectric (PE), DPHI and NPHI. Percentages of quartz, clay (in the form of Illite), calcite and porosity were calculated and plotted with respect to depth.

The Wood County well, API# 4710701266, was completed in 1983 in the Middle Devonian Oriskany Sandstone; however it was drilled through the Newburg and into the Upper Ordovician Juniata red beds. The Newburg in this well appears to have repetitive intervals of higher calcite deposition and higher quartz influx. Simultaneously, a steady influx of terrigeneous fine clay material is suggested throughout (Figure 5.5 a). Porosity does not show up on the composition plot and when the PHID and PHIN are averaged, this is reflected on the log. This is further reinforced by high density values throughout the interval. Although according to the analysis there is no porosity, any porosity that does exist is likely saturated with water (Figure 5.5 a, b).

The progradational parasequences previously described in the cored intervals is not seen in the Wood 1266 well log (API # 4710701266). A retrogradational sequence, capped by a maximum flooding surface (MFS), consisting of predominantly calcite, marks the transition from the McKenzie into the Newburg. This gradual flooding sequence continues through the entire Newburg interval in this area.

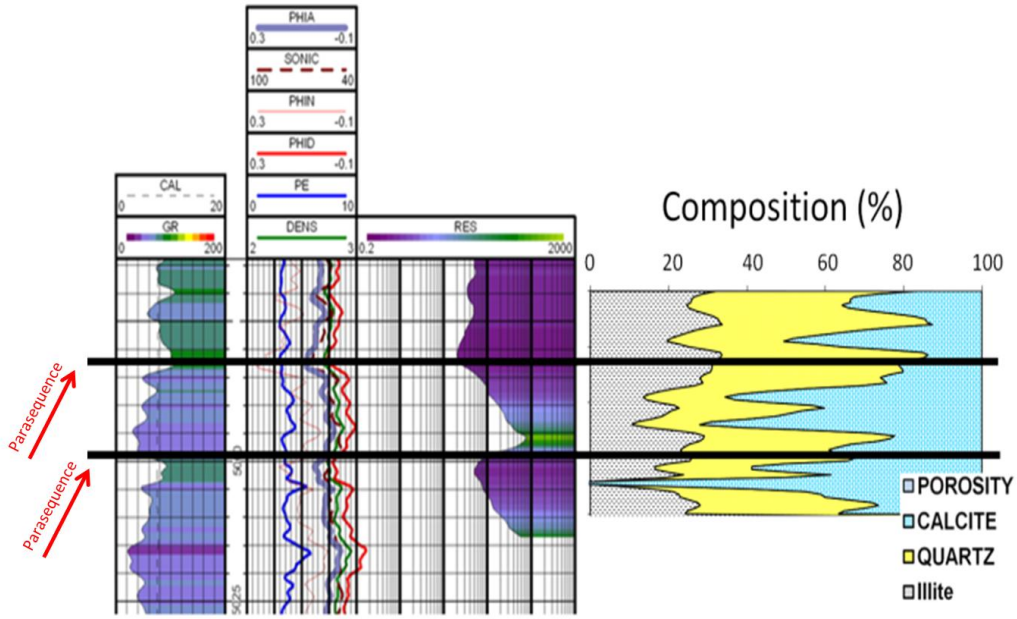

Figure 5.5 a

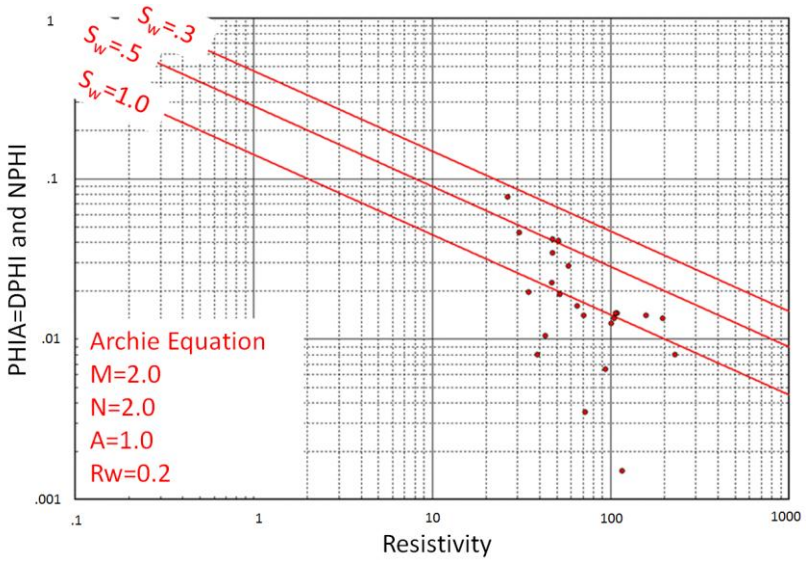

Figure 5.5 b

Figure 5.5 a. Log analysis of Wood 1266 (API # 4710701266). Compositional plot. **b.** Pickett plot. Red arrows on log (a.) indicate individual parasequences.

The Putnam County well, API# 4707901155, was completed in 1990 in the Upper Devonian Lower Huron Shale. In this well, porosity is difficult to determine from log analysis because of a lack of an NPHI log. Throughout the analyzed interval, the Newburg appears to be predominantly composed of quartz with a “stringer” of calcite towards the bottom of the Newburg. Density values decrease in the upper half of the interval, possibly due to pore space becoming saturated with water (Figure 5.6 a and b). This log shows the shoaling upward sequence typical of Newburg deposition.

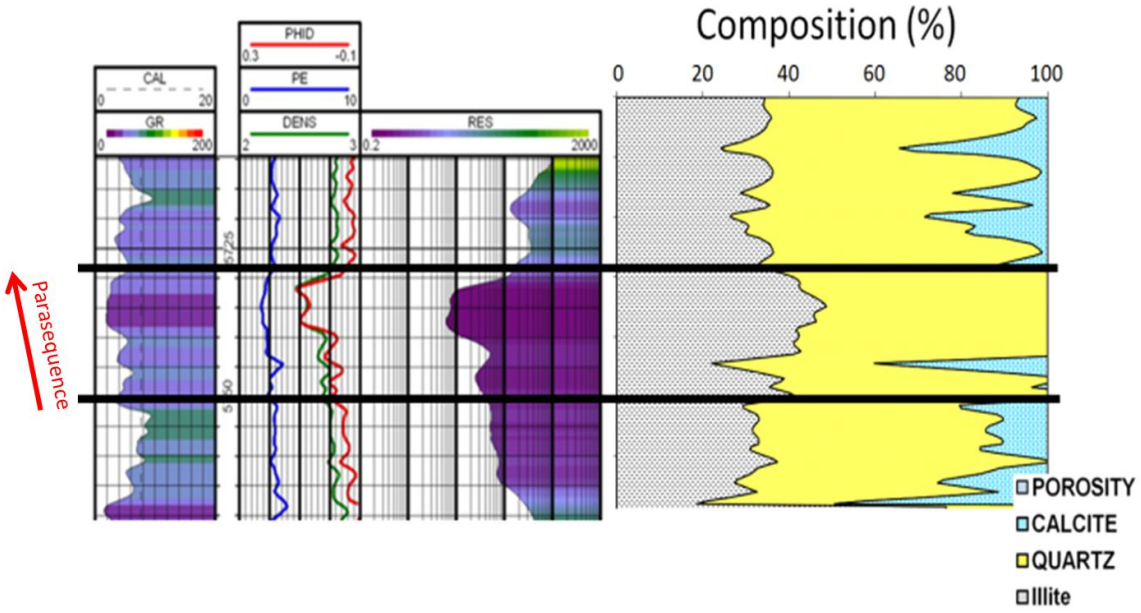

Figure 5.6 a

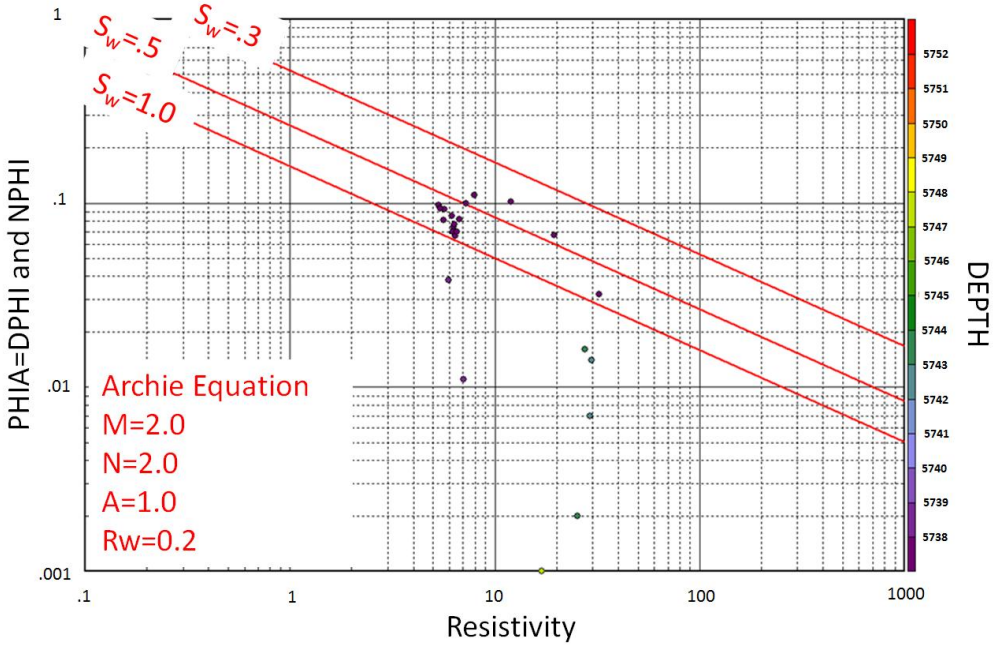

Figure 5.6 b

Figure 5.6 a. Log analysis of Putman #1155 (API# 4707901155). Compositional plot. **b.** Pickett plot. Red arrows on log (a.) indicate individual parasequences.

5.3 Modern Analogue

Sand-rich carbonate intervals with intermittent influxes of terrigeneous fines appear to have been consistently deposited throughout the Newburg interval, with finer material found in the Roane 714 well. In core, low energy sedimentary structures reinforce the idea of a restricted basin; however, repeated parasequences show the position of the shoreline was constantly changing.

A majority of the study area reflects consistent thicknesses throughout, with the exception of the two anomalies described in the north and south of the study area

(Figure 4.6). The southern anomaly could be a result of deposition or thrusting due to its proximity to the Taconic uplift. If the northern anomaly is interpreted as increased deposition, a barrier island model may be sufficient. However, as stated earlier, there is an abundance of repeated material due to thrusting as observed in the Sand Hill well (Cardwell, 1971). Assuming that these increases in thicknesses are a result of structural processes, a central-estuarine, tidal flat model may be adequate to describe deposition (Figure 5.7).

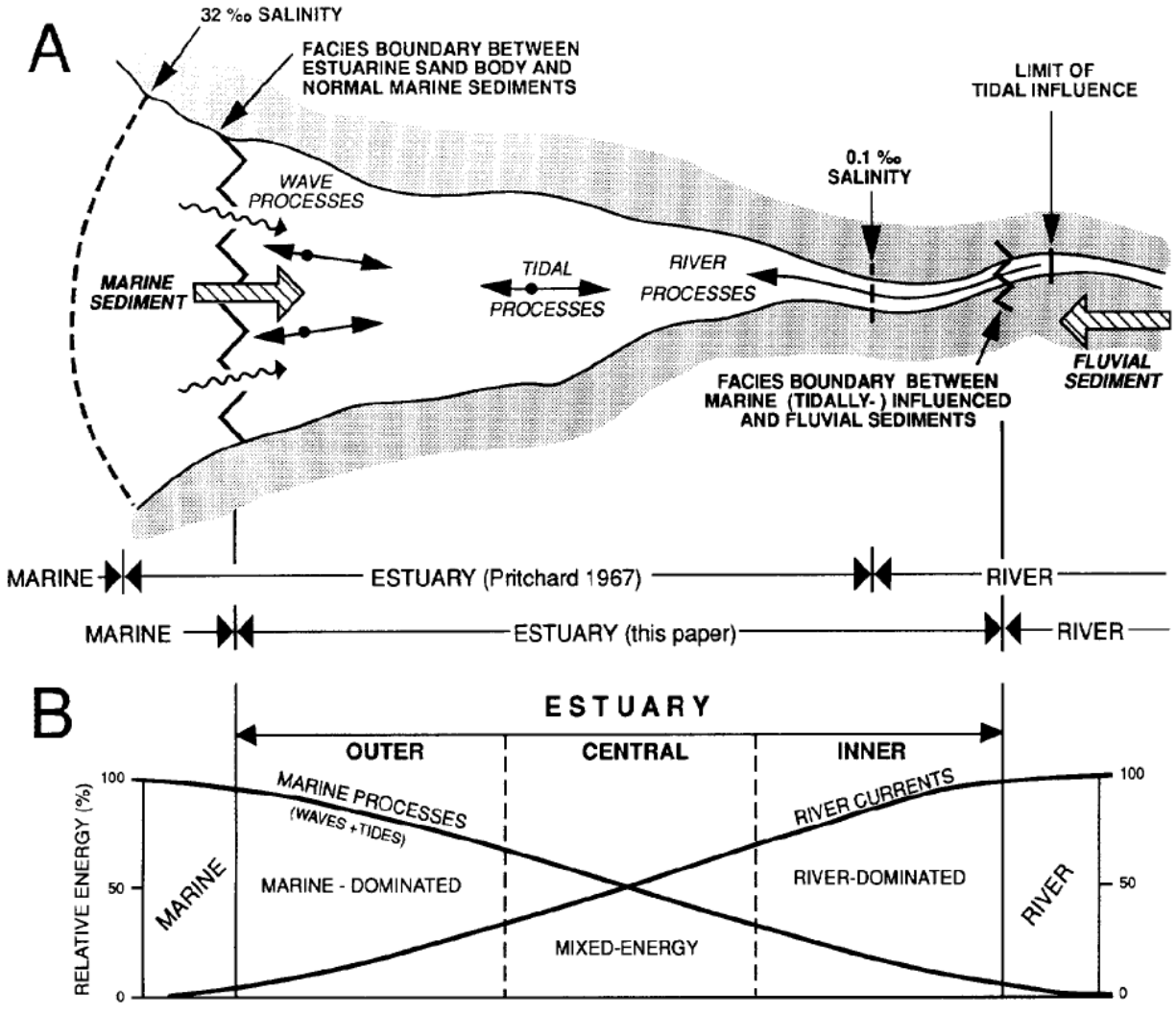

Figure 5.7 Estuarine depositional model (source: Dalrymple *et al.*, 1992).

Famous for its unique, present-day carbonate production, the Persian Gulf (Figure 5.8) is not known for its barrier islands. Instead, it is known for a shallow, sloping, carbonate ramp, and its location within a restricted basin. Sediments typically fine toward the basin and become coarser landward. There are typically no barriers to incoming ocean currents so energy offshore is low and gradually increases landward (Bathurst, 1975). In the Persian Gulf model, the finer grain size in the Roane 714 well, compared to the other cores, would place this well further offshore compared to the other cored wells.

Figure 5.8 Satellite image of Persian Gulf and surrounding region (Google Earth, 2011).

The Persian Gulf is also known for its high salinities and high evaporation rates. Gypsum appears in the western cores in the form of clasts and replacement of dolomite. The Roane 714 core appears to be free of gypsum and abundant in carbonate. The absence of evaporites in this well compared to the other cored wells to the west suggests an undulating shoreline was probably situated somewhere in between, during deposition of the Newburg (Figure 5.9).

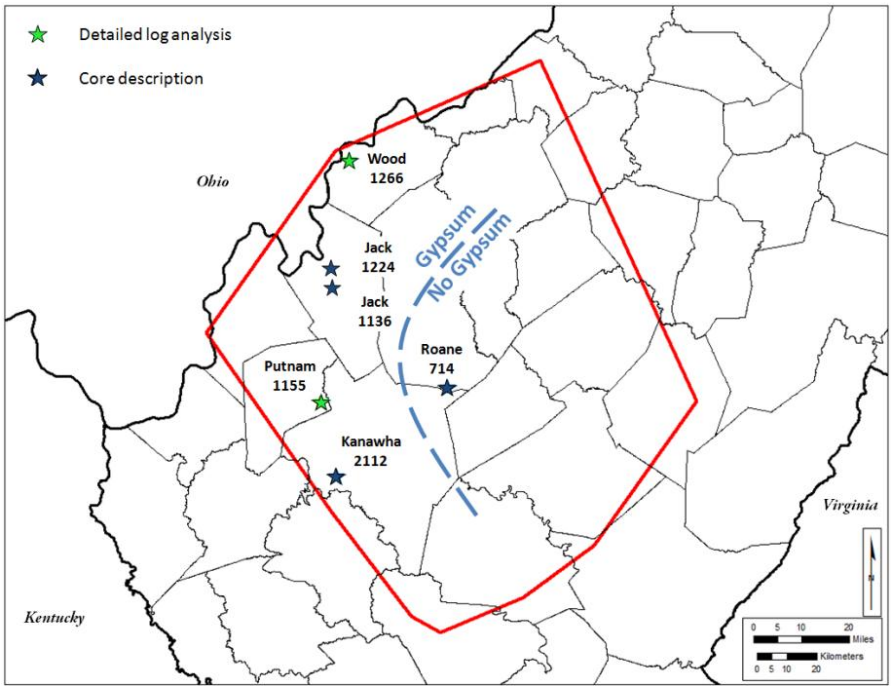

Figure 5.9 Map showing general accumulation of gypsum during Newburg deposition in the study area.

Intertidal and supratidal deposits were observed in all the cores implying that water depth throughout the study area ranged from zero to several feet (Figure 5.10). The lack of relief during deposition of the Newburg may imply that changes in sea level were most likely localized and not the result of eustacy. Dark shales in the Newburg could

be the result of relatively shallow, restricted environments, such as tidal pools or lagoons, where organic matter could accumulate without being degraded.

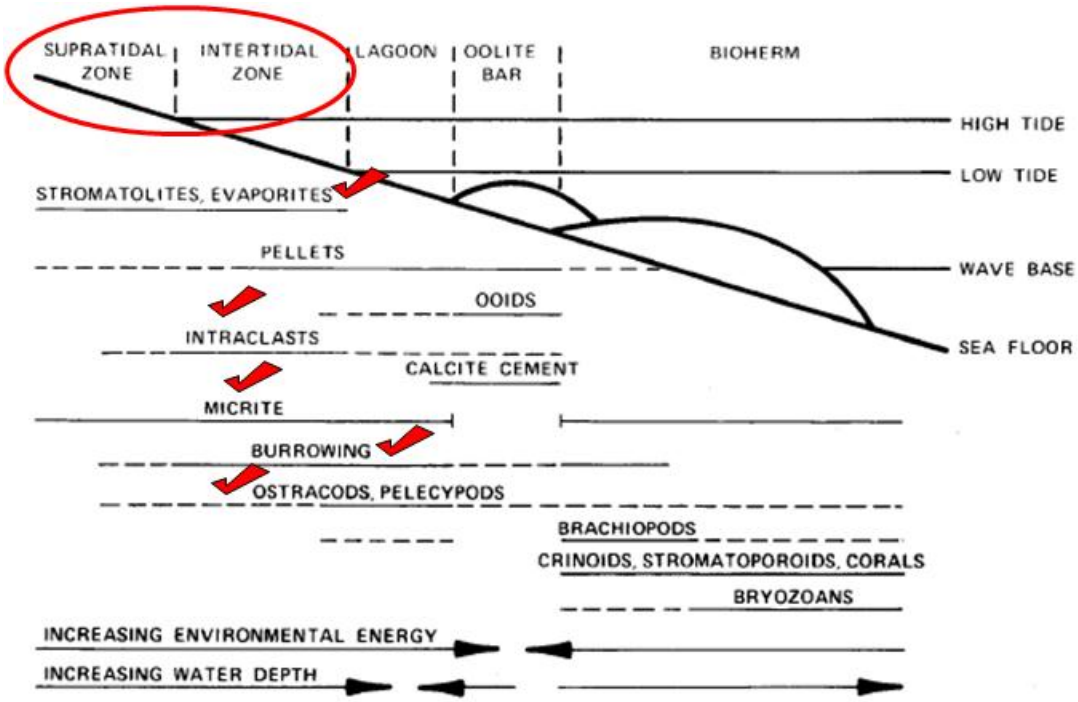

Figure 5.10 Depositional environments, energy levels and diagnostic criteria in Wayne County McKenzie core. Red checks represent evidence observed in core (Figure modified from Patchen and Smosna, 1975, p. 2274.)

The resulting depositional model for the Newburg could be a combination of the estuarine and carbonate ramp environments within a restricted basin, with wind and fluvial processes providing a majority of the oxygen and siliciclastics, while algae growth provided a majority of the organic material. Tidal channels probably accounted for any localized heterogeneity (Figure 5.11).

Figure 5.11 Coastline image of the Persian Gulf.

Source: *http://ourlifeinprague.wordpress.com/2011/09/23/desert-safari-part-1/*

Using the presence of gypsum in the core combined with the isopach maps, the restriction of the basin during deposition of the Newburg is interpreted. The isopach maps provide an idea of the tidal/subtidal boundary, otherwise known as the central mixing zone in the estuarine model (Dalrymple *et al.*, 1992). The lack of gypsum in the Roane County well indicates that this area was predominantly submerged during Newburg deposition. Gypsum became present in other locations later in the transition from the Newburg to the Salina (Figure 5.12).

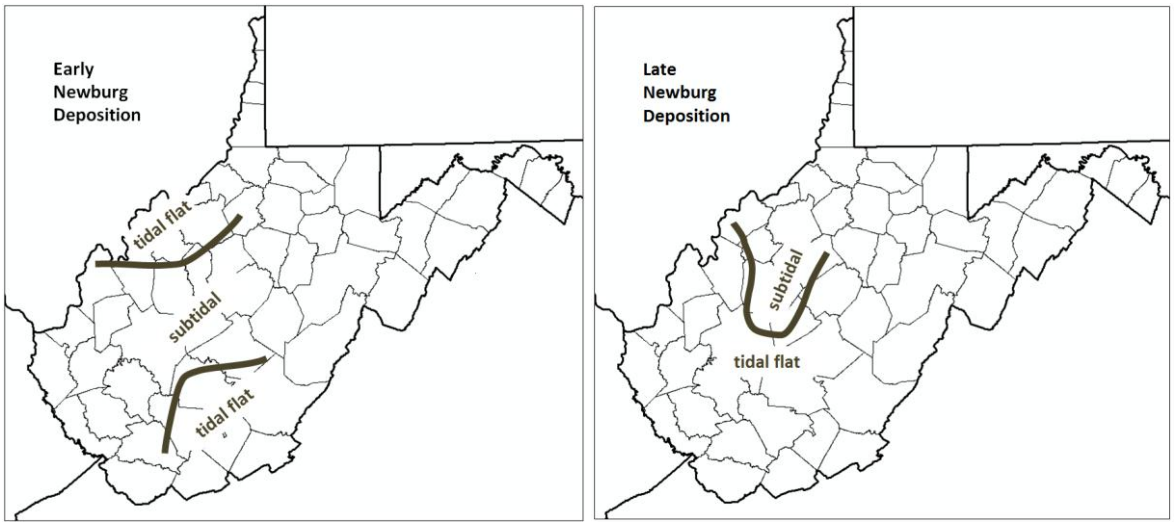

Figure 5.12 Interpreted restriction of the basin during deposition of the Newburg.

6.0 Conclusions

The Newburg appears to be adequate for small-scale injection tests in areas defined by fields where production has ceased; however, on a regional scale, porosity is not consistently high throughout the study area. Rather, it is limited to a few “sweet spots” that contain a highly porous zone within the formation. These sweet spots are defined by structural and stratigraphic traps associated with salt water contacts, generally confined to the south and west of the study area. The integrity of the seal appears to be more than adequate to retain CO_2, as evidenced by the high production pressures.

The results of porosity calculations were relatively surprising for a formation known for a pay zone with high production pressures and lack of cement. Because the porosity was calculated across the entire interval, finer-grained material deposited by migrating shorelines and fluvial systems offset the otherwise more highly porous beach sands. By computing porosity cutoffs, an attempt was made to compensate for this lack of porosity in an otherwise highly productive formation. In general, the defined porosity cutoffs mirrored the location of the North/South Ripley, Kanawha Forest and Coopers Creek fields. One reason for the poor definition of the fields could be due to poor well logging conditions through the pay zone reflecting a lack of cement; therefore, enlarging the well bore and creating a poor log signature (Patchen, personal communication 2011). Otherwise, outside of the defined production fields, well control remains an issue when refining the porosity maps.

A carbonate ramp model, with estuarine influence is proposed for the Newburg as an alternative to the barrier island model. Similar lithologies exist in all the cores, excluding the presence of gypsum in Roane 714. Another distinguishing characteristic in this well is the finer grain size compared to those in the other available cores. Finer-grained sands become more prevalent in this part of the study area.

Based on the analysis of core and well logs, the Newburg Sandstone generally appears to consist of two marine parasequences representing shoreline progradation. The thicker, second parasequence is responsible for providing most of the porosity and hydrocarbon reservoirs in the interval. This shoaling-upward sequence consistently exists in all the logs and core analyzed in this study except for the Wood 1266 well.

Examination of core, in conjunction with analysis of well logs, allows one to interpret a general regression of an epiric sea, which led to the late Silurian evaporite sequence. By interpreting the depositional sequences in a study area, a lack of well control can somewhat be compensated for.

Finally, previous descriptions have correlated the Newburg with the Williamsport Sandstone, previously referred to as the Crabbottom Sandstone; however, evaporite deposits identified in core appear to be more characteristic of those found in Wills Creek

outcrops. Therefore, it's possible the Newburg is more stratigraphically equivalent to portions of the Wills Creek Formation instead of the Williamsport Sandstone.

It appears that the Newburg Sandstone is appropriately suited for small-scale injection tests into individual, proven, exhausted production fields, rather than large scale, regional storage operations. Also, with the trend of utilization of CO_2 for enhanced recovery purposes becoming more dominant, the Newburg may be a good candidate for the enhanced recovery of natural gas. Brine disposal operations may also benefit from the unique characteristics of the Newburg. Nevertheless, it remains an interesting formation that should remain on one's radar for present and future trends in dealing with America's energy issues.

API #	County	Permit #	Latitude	Longitude	Elevation	Datum	Well Type	NEWBURG (MD)	MCKENZIE_FM (MD)	Avg. Porosity	POR-FT
4700501540	Boone	1540	38.198425	-81.673862	1226	Ground Level	Oil and Gas	5397.01	5411.21	0.01	0.58
4700702236	Braxton	2236	38.694798	-80.816288	1216	Ground Level	Dry w/ O&G Show	8106	8121	0.05	0.4
4701502644	Clay	2644	38.584923	-80.99678	1309	Ground Level	Gas	7769.79	7778	0.06	0.15
4701900106	Fayette	106	37.938721	-80.970422	2960	Ground Level	Dry w/ Gas Show	8606	8630	0	0.27
4701900176	Fayette	176	37.956844	-81.097035	1716	Ground Level	Dry	7265	7276	0	0.22
4701900241	Fayette	241	38.113797	-80.984957	2305	Ground Level	Dry	8007	8040	0.06	0.94
4701900474	Fayette	474	37.976162	-81.302667	1445	Ground Level	Gas	6937	6950	0.01	0.14
4701900572	Fayette	572	38.069084	-81.092331	1707	Ground Level	Dry	7446	7482.32	0.02	0.94
4702500022	Greenbrier	22	38.060096	-80.733278	3462	Ground Level	Dry	9365.85	9385.59	0	0.23
4703501131	Jackson	1131	38.790324	-81.769027	592	Ground Level	Gas	5401	5415	0.01	0.63
4703501133	Jackson	1133	38.789243	-81.753004	804	Ground Level	Gas	5612	5628	0.01	1.15
4703501136	Jackson	1136	38.810701	-81.742563	929	Ground Level	Dry	5712.3	5726.2	0.01	0.72
4703501140	Jackson	1140	38.804171	-81.729978	814	Ground Level	Dry	5703.53	5719.97	0.01	0.78
4703501161	Jackson	1161	38.922844	-81.697875	830	Kelly Bushing	Dry w/ Gas Show	5679.61	5689.52	0	0
4703501191	Jackson	1191	38.860453	-81.731423	740	Ground Level	Gas	5554	5571.7	0.04	1.81
4703501218	Jackson	1218	38.862311	-81.719693	870	Ground Level	Dry w/ O&G Show	5721.6	5736.01	0.03	1.51
4703501224	Jackson	1224	38.893876	-81.72485	679	Kelly Bushing	Gas	5452	5460.89	0.01	0.57
4703501244	Jackson	1244	38.886725	-81.751764	610	Ground Level	Gas	5293	5300.73	0.02	0.84
4703501247	Jackson	1247	38.900926	-81.741535	758	Ground Level	Dry w/ Gas Show	5470	5477.75	0	0

4703501248	Jackson	1248	38.865199	-81.760106	855	Ground Level	Gas	5490	5494	0.04	0.37
4703501257	Jackson	1257	38.906948	-81.712347	605	Kelly Bushing	Dry	5432	5436	0	0.09
4703501260	Jackson	1260	38.856176	-81.769395	915	Ground Level	Dry	5508.73	5518.76	0	0
4703501267	Jackson	1267	38.866816	-81.771001	858	Ground Level	Gas	5426	5430	0.01	0.39
4703501282	Jackson	1282	38.894461	-81.788229	815	Ground Level	Dry	5197	5209.89	0	0
4703501366	Jackson	1366	38.729784	-81.572248	915	Ground Level	Gas	6184	6201.79	0.06	1.2
4703501374	Jackson	1374	38.894714	-81.8054	637	Ground Level	Gas	4952.92	4961.42	0	0
4703501382	Jackson	1382	38.855593	-81.785467	774	Ground Level	Gas	5295.65	5304.72	0	0
4703501384	Jackson	1384	38.918804	-81.798041	712	Ground Level	Gas	5008.89	5020.18	0	0
4703501425	Jackson	1425	38.871605	-81.823518	657	Kelly Bushing	Dry w/ Gas Show	4960	4972.19	0.08	0.94
4703501517	Jackson	1517	38.823148	-81.676684	720	Ground Level	Gas	5772.15	5780.53	0.03	0.44
4703501532	Jackson	1532	38.972313	-81.732256	786	Ground Level	Gas	5269.93	5285.12	0.01	0
4703902094	Kanawha	2094	38.45142	-81.733715	1000	Ground Level	Gas	5709	5725.06	0.02	1.46
4703902098	Kanawha	2098	38.449508	-81.760297	680	Ground Level	Gas	5373	5385.14	0.02	1.03
4703902112	Kanawha	2112	38.267373	-81.69724	932	Ground Level	Gas	5422.58	5438.37	0.01	0.65
4703902117	Kanawha	2117	38.415907	-81.755598	1012	Ground Level	Dry w/ Gas Show	5697.39	5705.23	0	0.03
4703902143	Kanawha	2143	38.440877	-81.760546	800	Ground Level	Dry w/ Gas Show	5489	5498.71	0	0.19
4703902196	Kanawha	2196	38.472681	-81.681829	863	Spirit Level	Gas	5691	5712	0.02	1.2
4703902210	Kanawha	2210	38.460906	-81.650601	662	Ground Level	Water Injection	5554	5573	0.02	0.76
4703902213	Kanawha	2213	38.237047	-81.598071	943	Kelly Bushing	Dry w/ Gas Show	5399.32	5413.59	0.02	0.75

4703902223	Kanawha	2223	38.463979	-81.711319	942	Ground Level	Gas	5701	5725	0.01	0.27
4703902259	Kanawha	2259	38.443238	-81.707941	714	Ground Level	Dry	5500.31	5518.02	0	0.39
4703902277	Kanawha	2277	38.453057	-81.568861	710	Kelly Bushing	Gas	5563	5567.97	0.01	0.72
4703902314	Kanawha	2314	38.515653	-81.64497	671	Kelly Bushing	Gas	5555	5562.58	0.02	0.75
4703902331	Kanawha	2331	38.480959	-81.60315	755	Ground Level	Dry	5653	5673.11	0	0
4703902337	Kanawha	2337	38.510448	-81.622451	1057	Ground Level	Gas	5927	5936.35	0.02	1.06
4703902369	Kanawha	2369	38.52015	-81.60035	659	Ground Level	Dry w/ Gas Show	5569.71	5578	0	0.05
4703902408	Kanawha	2408	38.473306	-81.557384	725	Ground Level	Gas	5614	5623.05	0.02	1.13
4703902410	Kanawha	2410	38.480439	-81.560364	879	Ground Level	Gas	5769	5781.11	0.02	1.56
4703902420	Kanawha	2420	38.447824	-81.553281	789	Ground Level	Gas	5672	5675.45	0.01	0.27
4703902430	Kanawha	2430	38.475439	-81.57177	820	Ground Level	Gas	5713.54	5733.91	0	0.02
4703902433	Kanawha	2433	38.533351	-81.384259	888	Ground Level	Dry w/ Gas Show	6360.33	6384	0.01	3.09
4703902445	Kanawha	2445	38.488782	-81.565318	908	Ground Level	Gas	5812	5828	0.02	1.64
4703902447	Kanawha	2447	38.498057	-81.619142	910	Kelly Bushing	Gas	5768	5773.19	0.02	0.49
4703902481	Kanawha	2481	38.140543	-81.51483	1425	Kelly Bushing	Dry w/ Gas Show	6479.59	6496.11	0.01	0.9
4703902742	Kanawha	2742	38.323274	-81.405479	959	Ground Level	Dry w/ Gas Show	6072.76	6085.79	0.04	0.41
4703902743	Kanawha	2743	38.27256	-81.477083	848	Ground Level	Gas	5753.86	5772.19	0.03	0.67
4703902744	Kanawha	2744	38.194682	-81.431643	943	Ground Level	Dry w/ Gas Show	6204.91	6223	0.02	0.52
4703902751	Kanawha	2751	38.241836	-81.392308	717	Ground Level	Dry w/ Gas Show	6075.02	6104.2	0.04	1.2
4703902755	Kanawha	2755	38.356096	-81.349482	737	Ground Level	Dry	6061	6083.25	0	0.58

4703902796	Kanawha	2796	38.051529	-81.451351	1120	Ground Level	Gas	6576.26	6593.12	0.01	0.61
4703903351	Kanawha	3351	38.372789	-81.458565	1290	Ground Level	Gas	6262.59	6281.24	0	0.32
4703903373	Kanawha	3373	38.352762	-81.559008	1085	Ground Level	Gas	5888	5909	0	0.45
4703903401	Kanawha	3401	38.366655	-81.440236	1315	Ground Level	Gas	6265	6282	0.02	0.35
4703903646	Kanawha	3646	38.280031	-81.454408	1381	Ground Level	Dry w/ Gas Show	6391	6424	0.03	1.8
4703903762	Kanawha	3762	38.314289	-81.459094	1462	Ground Level	Gas	6289	6301.99	0.03	1.01
4703903796	Kanawha	3796	38.035102	-81.403257	1334	Kelly Bushing	Gas	6888.15	6908	0	0.06
4703903883	Kanawha	3883	38.296449	-81.464063	1328	Ground Level	Gas	6207.27	6226.44	0.03	1.34
4703903896	Kanawha	3896	38.318349	-81.477688	1288	Ground Level	Gas	6059.03	6069.94	0.02	0.69
4703903908	Kanawha	3908	38.255105	-81.482544	748	Ground Level	Gas	5725.08	5747.49	0.03	1.81
4703903914	Kanawha	3914	38.283177	-81.529793	1459	Ground Level	Gas	6026.91	6053.31	0.03	2.33
4703903937	Kanawha	3937	38.321862	-81.499138	742	Ground Level	Gas	5513.47	5525.83	0.02	0.85
4703903950	Kanawha	3950	38.291188	-81.483386	1431	Ground Level	Gas	6164	6187.41	0.03	1.78
4703903963	Kanawha	3963	38.275813	-81.496259	1461	Ground Level	Gas	6168	6191	0.03	1.83
4703903970	Kanawha	3970	38.262615	-81.502416	1426	Ground Level	Gas	6155.9	6184	0.03	1.88
4703904353	Kanawha	4353	38.295288	-81.50297	1352	Ground Level	Gas	6029.08	6052	0.02	1.3
4703905404	Kanawha	5404	38.524789	-81.734585	801	Ground Level	Gas	5637.9	5654.19	0	0.18
4705300266	Mason	266	38.788181	-81.993455	788	Ground Level	Gas w/ Oil Show	4587.25	4594.14	0	0.13
4705300316	Mason	316	38.701165	-82.177083	558	Ground Level	Gas	3838.27	3844.3	0.03	0.34
4707900726	Putnam	726	38.469925	-81.727185	628	Ground Level	Gas	5377	5385.24	0.07	0.89

4707900737	Putnam	737	38.558081	-82.017448	687	Ground Level	Dry w/ Gas Show	4889.67	4901.13	0.04	0.84
4707900747	Putnam	747	38.61131	-81.84853	896	Ground Level	Dry	5598.11	5614.27	0	0
4707900762	Putnam	762	38.616726	-81.758635	702	Ground Level	Dry	5584	5601.6	0	0.18
4707900763	Putnam	763	38.547874	-81.768838	703	Ground Level	Dry	5536.23	5548.34	0.01	0.09
4707900782	Putnam	782	38.474571	-81.766396	812	Ground Level	Gas	5482	5496	0	0.2
4708100289	Raleigh	289	37.828802	-81.310142	1798	Ground Level	Gas	7221.32	7237	0	0.04
4708100336	Raleigh	336	37.871627	-81.384702	2247	Ground Level	Dry w/ Gas Show	7584.24	7599.4	0	0.06
4708100342	Raleigh	342	37.967743	-81.453858	1532	Ground Level	Gas	6907.57	6918.94	0	0.07
4708100688	Raleigh	688	37.865969	-81.1634	2045	Ground Level	Gas	7619	7636.49	0	0.23
4708701676	Roane	1676	38.774041	-81.214999	846	Ground Level	Gas w/ Oil Show	6866.76	6883.8	0	0.09
4708703197	Roane	3197	38.896766	-81.418598	713	Ground Level	Dry w/ Gas Show	6381.86	6386.74	0	0
4708704261	Roane	4261	38.660088	-81.239802	1020	Ground Level	Gas	6850.66	6866.78	0.09	1.27
4708704381	Roane	4381	38.718236	-81.42483	1063	Ground Level	Gas	6783.6	6797.71	0.04	0.48
4709501121	Tyler	1121	39.496161	-80.944384	742	Ground Level	Dry	7594.26	7613.07	0.06	1.09
4710100055	Webster	55	38.504066	-80.364696	1625	Ground Level	Dry w/ Gas Show	7496.69	7507.57	0.02	0.24
4710500725	Wirt	725	38.975725	-81.298996	902	Ground Level	Gas	6180	6215	0.01	0
4710500746	Wirt	746	38.945715	-81.365248	1106	Ground Level	Dry w/ Gas Show	6894.16	6908.16	0.08	1.77
4710500870	Wirt	870	38.951745	-81.398615	662	Ground Level	Dry	6451.39	6463.41	0	0.01
4710700594	Wood	594	39.119558	-81.67244	777	Ground Level	Dry	5265.52	5278.87	0	0
4710700598	Wood	598	39.203751	-81.620322	732	Ground Level	Dry	5301.96	5316.41	0	0
4710700803	Wood	803	39.115362	-81.498759	730	Kelly Bushing	Dry	5923.79	5939.09	0.03	0
4710701266	Wood	1266	39.223537	-81.658409	612	Kelly Bushing	Gas	4982.95	5000.1	0.03	0.49
4710701631	Wood	1631	39.120147	-81.676198	701	Ground Level	Gas	5177.69	5190.43	0	0

REFERENCES

Asquith, G. and D. Krygowski, 2004, Basic Well Log Analysis (Second Edition), American Association of Petroleum Geologists, Methods in Exploration Series No. 16, p. 40.

Bathurst, R., 1975, Trucial Coast Embayment, Carbonate Sediments and Their Diagenesis, p. 178-202.

Blakey, R., 2011, Northern Arizona University Geology, Paleogeography and Geologic Evolution of North America, <http://jan.ucc.nau.edu/~rcb7/nam.html> Accessed December 13, 2012.

Cardwell, D., 1971, The Newburg of West Virginia, West Virginia Geological and Economic Survey, Bulletin 35, p. 54.

Ciferno, J., J. Litynski, and S. Plasynski, 2010, Department of Energy/National Energy and Technology Laboratory Carbon Dioxide Capture and Storage RD&D Roadmap, p. 5.

Conti, J., P. Holtberg, J. Beamon, S. Napolitano, A. Schaal, and J. Turnure, 2012, Annual Energy Outlook 2012 with Projections to 2035, United States Department of Energy, Energy Information Agency, p. 4.

Conway, T. and P. Tans, 2012, National Oceanic and Atmospheric Administration, <www.esrl.noaa.gov/gmd/ccgg/trends/global.html> Accessed November 25, 2012.

Dalrymple, R., B. Zaitlin, and R. Boyd, 1992, Estuarine Facies Models: Conceptual Basis and Stratigraphic Implications, Journal of Sedimentary Petrology 62, p.1130-1146.

Diecchio, R. and J. Dennison, 1996, Silurian Stratigraphy of Central and Northern Virginia and Adjacent West Virginia, Sedimentary Environments of Silurian Taconia – Fieldtrips to the Appalachians and Southern Craton of Eastern North America, Prepared for the Pre-Conference Field Trip of the 2nd International Symposium on the Silurian System, University of Tennessee, Department of Geological Sciences, Studies in Geology 26, p. 107-127.

Department of Energy/National Energy and Technology Laboratory, 2010, Carbon Sequestration Atlas of the United States and Canada, Third Edition, p. 27.

Gao, D. and R. Shumaker, , 1996, Subsurface Geology of the Warfield Structures in Southwestern West Virginia: Implications for Tectonic Deformation and Hydrocarbon Exploration in the Central Appalachian Basin, American Association of Petroleum Geologists Bulletin, v. 80, p.1242-1261.

Gibbins, J. and H. Chalmers, 2008, Carbon Capture and Storage, Energy Policy, v. 36, p. 4317-4322.

Haught, O., 1959, Oil and Gas in Southern West Virginia: West Virginia Geological and Economic Survey, Bulletin 17.

IEA, 2012, World Energy Outlook 2012, International Energy Agency, <http://www.worldenergyoutlook.org/> Accessed November 25, 2012.

Kamola, D. and J. Van Wagoner, 1995, Stratigraphy and Facies Architecture of Parasequences with Examples from the Spring Canyon Member, Blackhawk Formation, Utah, American Association of Petroleum Geologists Memoir 64, Sequence Stratigraphy of Foreland Basin Deposits, p. 27-54.

Lytle, W., T. DeBrosse, E. Bendler, W. Bushman, A. Johnson, J. Edwards Jr., d. Young, and D. Patchen, 1972, Oil and Gas Developments in Maryland, Ohio, Pennsylvania, Virginia, and West Virginia, p. 1310 - 1328, v. 56, Issue 7. (July).

Lytle, W., J. Edwards Jr., T. DeBrosse, E. Bendler, A. Johnson, W. Bushman, R. Loper, and D. Patchen, 1973, Oil and Gas Developments in Maryland, Ohio, Pennsylvania, Virginia, and West Virginia, p. 1548 - 1570, v. 57, Issue 8. (August).

Lytle, W., J. Edwards Jr., T. DeBrosse, E. Bendler, A. Johnson, W. Bushman, K. Roane, R. Loper, and D. Patchen, 1974, Oil and Gas Developments in Maryland, Ohio, Pennsylvania, Virginia, and West Virginia, p. 1640 - 1661, v. 58, Issue 8. (August).

Lytle, W., J. Edwards Jr., T. DeBrosse, K. Roane, E. Bendler, W. Bushman, W. Kelley, and D. Patchen, 1975, Oil and Gas Developments in Maryland, Ohio, Pennsylvania, Virginia, and West Virginia, p. 1438 - 1470, v. 59, Issue 8. (August).

Lytle, W., J. Edwards Jr., T. DeBrosse, K. Roane, E. Bendler, J. Hermann, W. Kelley, and D. Patchen, 1976, Oil and Gas Developments in Maryland, Ohio, Pennsylvania, Virginia, and West Virginia, p. 1288 - 1322, v. 60, Issue 8. (August).

Lytle, W., J. Edwards Jr., T. DeBrosse, E. Bendler, J. Hermann, W. Kelley, and D. Patchen, S. Brock, 1977, Oil and Gas Developments in Maryland, Ohio, Pennsylvania, Virginia, and West Virginia, p. 1269 - 1304, v. 61, Issue 8. (August).

McArdle, P., P. Lindstrom, M. Mondshine, S. Calopedis, N. Checklick, and S. Goldstein, 2002, Emissions of Greenhouse Gases in the United States 2001, Department of Energy/Energy Information Agency, DOE/EIA-0573 (2001), ES2/Table 4.

McDowell, R., K. Avary, J. Lewis, J. Britton, P. Hunt, P. Waggy, and M. Ganak, 2007a, Preliminary Bedrock Map of the Milam Quadrangle: West Virginia Geological and Economic Survey Open File Publication, OF-0602.

McDowell, R., K. Avary, J. Lewis, J. Britton, P. Hunt, P. Waggy, and M. Ganak, 2007b, Preliminary Bedrock Map of the Cow Knob Quadrangle: West Virginia Geological and Economic Survey Open File Publication, OF-0603.

Metz, B., O. Davidson, H. de Coninck, M. Loos, and L. Meyer, 2005, Intergovernmental Panel on Climate Change, Special Report on Carbon Dioxide Capture and Storage Cambridge University Press, Cambridge, United Kingdom and New York.

MRCSP, 2010, How Does Geologic Storage of Carbon Dioxide Work?, Midwest Regional Carbon Sequestration Partnership, http://216.109.210.162/userdata/Fact%20Sheets/howgeostorage.pdf, accessed July 23, 2012.

NATCARB, 2012, United Sates Department of Energy/National Energy and Technology Laboratoryhttp://natcarbviewer.com/, accessed November 27, 2012.

NGMDB, 2012, National Geologic Map Database, U.S. Department of the Interior, U.S. Geological Survey, <http://ngmdb.usgs.gov/Geolex/geolex_home.html> Accessed November 21, 2012.

NIST, 2011, Thermophysical Properties of Fluid Systems, National Institute of Standards and Technology, <http://webbook.nist.gov/chemistry/fluid/> Accessed July 12, 2012.

Overbey, W., 1961, Oil and Gas Report on Jackson, Mason and Putnam Counties, West Virginia: West Virginia Geological and Economic Survey, Bulletin 23, p 26.

Patchen, D., 1967, Newburg Gas Development in West Virginia – Preliminary Report, West Virginia Geological and Economic Survey, Circular 6, p. 1-31.

Patchen, D., and R. Smosna, 1975, Stratigraphy and Petrology of Middle Silurian McKenzie Formation in West Virginia, American Association of Petroleum Geologists, Bulletin v. 59, No. 12, p. 2266-2287.

Patchen, D., K. Schwarz, T. DeBrosse, E. Bendler, J. Hermann, L. Heyman, C. Cozart, W. Kelley, and D. Patchen, 1978, Oil and Gas Developments in Maryland, Ohio, Pennsylvania, Virginia, and West Virginia, p. 1399 - 1440, v. 62, Issue 8. (August).

Patchen, D., K. Schwarz, T. DeBrosse, E. Bendler, J. Hermann, R. Piotrowski, C. Cozart, and W. Kelley, 1979, Oil and Gas Developments in Maryland, Ohio, Pennsylvania, Virginia, and West Virginia in 1978, p. 1244 - 1277, v. 63, Issue 8. (August).

Patchen, D., K. Schwarz, T. DeBrosse, E. Bendler, J. Hermann, R. Piotrowski, and W. Kelley, 1980, Oil and Gas Developments in Maryland, Ohio, Pennsylvania, Virginia, and West Virginia in 1979, p. 1403 - 1436, v. 64, Issue 9. (September).

Patchen, D., K. Schwarz, T. DeBrosse, E. Bendler, J. Hermann, J. Harper, W. Kelley, and K. Avary, 1981, Northeastern United States, p. 1896 - 1929, v. 65, Issue 10. (October).

Patchen, D., K. Schwarz, T. DeBrosse, E. Bendler, M. McCormac, J. Harper, W. Kelley, and K. Avary, 1982, Oil and Gas Developments in Maryland, Ohio, Pennsylvania, Virginia, and West Virginia in 1981, p. 1955 - 1998, v. 66, Issue 11. (November).

Patchen, D., K. Schwarz, T. DeBrosse, E. Bendler, M. McCormac, J. Harper, W. Kelley, and K. Avary, 1983, Oil and Gas Developments in Mid-Eastern States in 1982, p. 1570 - 1592, Volume 67, Issue 10. (October).

Patchen, D., K. Schwarz, T. DeBrosse, E. Bendler, M. McCormac, J. Harper, W. Kelley, and K. Avary, 1984, Oil and Gas Developments in Mid-Eastern States in 1983, p. 1383 - 1399, v. 68, Issue 10. (October).

Patchen, D., K. Schwarz, T. DeBrosse, E. Bendler, M. McCormac, J. Harper, W. Kelley, and K. Avary, 1985, Oil and Gas Developments in Mid-Eastern States in 1984, p. 1518 - 1533, v. 69, Issue 10. (October).

Patchen, D., K. Schwarz, T. DeBrosse, E. Bendler, M. McCormac, J. Harper, W. Kelley, and K. Avary, 1986, Oil and Gas Developments in Mid-Eastern States in 1985, p. 1259 - 1272, v. 70, Issue 10. (October).

Patchen, D., K. Schwarz, T. DeBrosse, M. McCormac, J. Harper, W. Kelley, and K. Avary, 1987, Oil and Gas Developments in Mid-Eastern States in 1986, p. 88 - 101, v. 71, Issue 10B. (October Part B).

Patchen, D., K. Schwarz, T. DeBrosse, M. McCormac, J. Harper, W. Kelley, and K. Avary, 1988, Oil and Gas Developments in Mid-Eastern States in 1987, p. 88 - 103, v. 72, Issue 10B. (October Part B).

Patchen, D., K. Schwarz, M. McCormac, J. Harper, C. Cozart, W. Kelley, and K. Avary, 1989, Oil and Gas Development in Mid-Eastern States in 1988, p. 87 - 104, v. 73, Issue 10B. (October Part B).

Patchen, D., K. Schwarz, M. McCormac, J. Harper, C. Cozart, W. Kelley, and K. Avary, 1990, Oil and Gas Developments in Mid-Eastern States in 1989, p. 89 - 106, v. 74, Issue 10B. (October Part B).

Patchen, D., 1996, The Atlas of Major Appalachian Gas Plays, PLAY Sns: The Upper Silurian Newburg Sandstone Play, West Virginia Geological and Economic Survey, v. 25, p. 139-144.

Reger, D. and R. Tucker, 1924, Mineral and Grant Counties, West Virginia Geological and Economic Survey, County Geologic Report 16.

Russel, W., 1972, Pressure-depth Relations in Appalachian Region: American Association of Petroleum Geologists Bulletin, v. 56, p. 528-536.

Swartz, C. and F. Swartz, 1940, Silurian of the Central Appalachians, Geological Society of America Bulletin, abstract, v. 51, No. 12, p. 2008-2009.

Skeen, J., 2009, Basin Analysis and Aqueous Chemistry of Fluids in the Oriskany Sandstone, Appalachian Basin, USA, Master's thesis, West Virginia University.

Smosna, R., and D. Patchen, 1978, Silurian Evolution of Central Appalachian Basin, American Association of Petroleum Geologists Bulletin v. 62, No.11, p. 2308-2328.

Stout, W., R. Lamborn, D. Ring, J. Gillespie, and J. Lockett, 1935, Natural Gas in Central and Eastern Ohio, in Ley, H.A., ed., Geology of Natural Gas: Tulsa, OK, American Association of Petroleum Geologists, p. 897-914.

Tissot, B., and D. Welte, 1978, Petroleum Formation and Occurrence, p. 260.

Woodward, H., 1941, Silurian System of West Virginia, West Virginia Geological and Economic Survey, v.14, p. 1-300.

USDOE, 2012, The United States Carbon Utilization and Storage Atlas, Fourth Edition, United States Department of Energy/National Energy Technology Laboratory, p. 130.

USGS, 2012, National Geologic Map Database (NGMDB), Geologic Names Lexicon, United States Geological Survey, <http://ngmdb.usgs.gov/Geolex/> Accessed November 18, 2012.

Woodward, H., 1959, General Stratigraphy of the Area, in A Symposium on the Sandhill Deep Well, Wood County, West Virginia: West Virginia Geological and Economic Survey, Report of Investigations, No. 18, p. 1-182.

WVCARB, 2008, West Virginia Carbon Sequestration, <http://www.wvcarb.org/cc-overview.php> Accessed July 23, 2012.

WVGES, 2005, Phase 1 dataset prepared to aid in determining CO_2 sequestration on a field by field basis, West Virginia Geological and Economic Survey.

WVGES, 2012, Stratigraphic chart, “Major Rock Units of West Virginia”, West Virginia Geological and Economic Survey, unpublished.

WVGES database, updated 2012, WVGES Oil and Gas Well Data for West Virginia, West Virginia Geological and Economic Survey, publication DDS-5, <http://www.wvgs.wvnet.edu/www/news/datacd.htm> Accessed July 23, 2012.